Evaluation of Vehicle Positioning Accuracy using GPS-Enabled Smartphones in Traffic Data Capturing

by

Na Yin

A thesis submitted in partial fulfillment of the requirements for the degree of

Master of Science
in
Transportation Engineering

Department of Civil and Environmental Engineering
University of Alberta

ABSTRACT

Connected Vehicle (CV) technology aims to improve transportation management and system performance by incorporating advanced detection and communication system such as Global Positioning System (GPS), and smart devices to make roads and vehicles better equipped to exchange important information regarding road and travel conditions. GPS have emerged as the leading technology to provide location information to various location based services. With an increasing smartphone penetration rate, as well as expanding spatial and network coverage, the idea of combining GPS positioning functions with smartphone platforms to perform GPS-enabled smartphone-based traffic management and data monitoring is promising. This study presents a field experiment conducted along Whitemud Drive (a section of Connected Vehicle Test Bed in Edmonton, Alberta, Canada), Queen Elizabeth Highway, and various urban arterial roadways using a GPS-enabled smartphone, cellular positioning technique, professional GPS handset and combination of smartphone and Geofence. The relative positioning errors and the data collection performances using the aforementioned technologies were evaluated and compared. The characteristics and the relationships between the positioning errors and traffic related factors are investigated using regression analysis. The results indicate that GPS-enabled smartphones are capable of correctly positioning 92% of the roadway segments to Google Earth, while achieving accuracy of less than 10 meters for 95% of the data. Using a cellular positioning technique, cell-IDs were correctly identified in

repeatable trials with accuracy levels much lower than the smartphone-GPS positioning. Using combination of smartphone positioning and Geofence are promising in finding accurate positions and timestamps. In all scenarios, the use of four data source for obtaining location and traffic condition is feasible; and particularly, using GPS-enabled smartphones and/or its combination with Geofences can provide good accuracy level for location and traffic state parameter estimates.

ACKNOWLEDGEMENT

I would like to express the deepest appreciation to my supervisor Dr. Zhijun Qiu for the continuous support of my study and research for his patience, motivation, and immense knowledge. It has been a memorable and delightful experience for me to work in Dr. Qiu's research group. I would like to thank my other committee members: Dr. Amy Kim and Dr. Arturo Sanchez-Azofeifa for their support, encouragement, and insightful comments.

I would like to thank my dear research teammates in Center of Smart Transportation: Dr. Pengfei Li, and Dr. Jie Fang, who are knowledgeable and resourceful, for their valuable suggestions and supports; Gang Liu, Xu Wang, Chen Lan, Ying Luo, Xu Han, Lin Shao, Jing Cao, Michael Ge, Dr. Hui Zhang, Dr. Mingjun Liao, Dr. Md Hadiuzzaman, and Md Ahsanul Karim, for the stimulating discussions, valuable suggestions and generous help in research and graduate studies. Furthermore I would also like to thank Rochelle Borchman and Jeffrey King for providing great comments and their patient help in writing academic papers and reports.

My sincere thanks also go to my dear colleges in Alberta Transportation for their patience, support and valuable advices. Special thanks to Fred Ko, Brian Mofford, Marie Ordano, Marc Audy, Cameron Lee, and Tiago Silva from the Intelligent Imaging Systems for providing the Geofence data.

Last but not least, I wish to express my deepest love to my dearest family members for their love, understanding and support for all these years.

TABLE OF CONTENTS

LIST OF TABLES

LIST OF FIGURES

LIST OF ABBREVIATIONS

ITS	Intelligent Transportation System
CV	Connected Vehicle
GPS	Global Positioning System
GSM	Global System for Mobiles
AGPS	Assisted Global Positioning System
WMD	Whitemud Drive
QEII	Queen Elizabeth Highway 2
WB	Westbound
EB	Eastbound
AVI	Automatic Vehicle Identification
AVL	Automatic Vehicle Location
SA	Selective Availability
AGPS	Assisted GPS
GNSS	Global Navigation Satellite System
HRMS	Horizontal Root Mean Square
ANOVA	Analysis of Variance
HDOP	Horizontal Dilution of Precision
RSSI	Receiver Signal Strength Indicator
AIC	Akaike's Information Criterion
BIC	Sawa's Bayesian Information Criterion
SBC	Schwarz's Bayesian Information Criterion

CHAPTER 1. INTRODUCTION

This chapter introduces the background of the GPS based mobile probe technology and their importance to traffic monitoring and management systems. The state and problems of current applications are described and study motivations as well as structure of thesis is presented.

1.1 Background

Traffic congestion and road safety issues impose costs on the society and economy and generate multiple impacts on urban region and their inhabitants. With understanding of these problems, transportation researchers have focused their efforts on implementing the Intelligent Transportation System (ITS) to improve mobility and safety while maintaining a sustainable transportation environment. As the latest development in ITS, Connected Vehicle (CV) technology presents a new multidisciplinary area incorporating advanced detection and communication system such as Global Positioning System (GPS), and smart devices to make roads and vehicles better equipped to exchange important information regarding road and travel conditions [1]. Several wireless communication technologies have been under development in parallel with CV advances and the smart device-based CV applications seem especially promising due to high penetration rate and relatively low cost.

Global Positioning Systems (GPS), which facilitate operational simplicity, accuracy and reliability for the transportation industry, have emerged as the leading technology to provide location information for various services, such as

navigation, commercial, emergency and networking. Improvements in GPS receiver technology have resulted in reliable and affordable GPS receivers for a wide range of applications. In recent years, GPS and cellular probe techniques have been researched and practiced in academic and industrial areas all around the world [2] [3]. In the era of mobile internet services, industries have a growing interest in using probe-based monitoring systems in the field of traffic data capturing. With an increasing smartphone penetration rate [4], as well as expanding spatial and network coverage, the idea of combining GPS positioning functions and smartphone platforms to perform GPS-enabled smartphone-based traffic management and data monitoring is promising and has recently attracted much research attention. Most smartphone come equipped with GPS as a standard feature. Leveraging this, we can glean accurate location information and traffic data from devices that are already deployed and in use. Increased data resources and data quality will improve the management in transportation planning and operation, thus providing better service to the road users.

Smartphone based CV applications rely on the GPS positioning function provided in most smart devices, therefore, the positioning accuracy of GPS-enabled smartphones is crucial to the development and performance of the CV application, and uncertainties regarding to the position accuracy need to be resolved. Under normal circumstances, the standard deviation of a non-differential GPS position estimate, which is typical in smart personal devices is in the order of 10 to 20 meters (m) [5] [6]. However, there are circumstances where GPS is unable to meet these requirements. Tall trees and buildings along the road

segment may impede the line-of-sight of GPS receivers to at least four satellites, and the accuracy of the calculated position depends on the changing geometry of the satellites in view and on the amount of multi-paths, which result from the surrounding environment [7].

1.2 Problem Statement and Research Motivation

It is anticipated that these above mentioned circumstances will be encountered when using GPS-enabled smartphones as probe devices for traffic data collection and condition monitoring. First, the GPS-enabled smartphones are in-vehicle, so the location accuracy will be lower than the case where a GPS receiver mounted on the top of a vehicle. Second, as GPS-enabled smartphones are often used in urban areas, tall trees and buildings cannot be avoided, thereby, blocking the line-of-sight between the GPS and four satellites. Furthermore, the multipath effect caused by urban canyon reflections will also exist. Third, the aforementioned level of accuracy is estimated in static mode and at fixed measuring location; positioning accuracy estimated with a moving smartphone GPS receiver in different transportation modes may be different. There are a few problems regarding to the positioning accuracy need to be looked at: The positioning accuracy estimated with a moving smartphone GPS receiver in mobile mode need to be quantified, the characteristics of the positioning error and the impact of traffic related factors on the positioning error is not well understood; and the feasibility of deploying a combination of location based data capturing techniques in City of Edmonton is unknown.

With the increasing number of available data sources, researchers are looking forward to make use of those data, and understanding the fundamentals of the data is crucial. In order to have a better understanding on the impact of aforementioned uncertainties and issues of using GPS-enabled smartphones as traffic management measures, this research conducts field experiments to first estimate the GPS-enabled smartphone positioning accuracy in the mobile states, then compare the performances of several position estimation technologies, and also investigate relationships between traffic related factors and positioning accuracy, as well as estimate the impact of these factors on accuracy of the traffic data.

In contrast to most GPS accuracy studies that focus on estimating positioning accuracy using professional GPS devices in static mode at fixed positions, this study focuses on estimating the relative positioning error among four data sources listed below using different technologies and devices in a moving vehicle. The relative positioning error using different technologies and their performances on different roadway facilities in City of Edmonton, as well as the relationships between the traffic related factor and the positioning error will be quantified. It is anticipated that a better understanding of smartphone GPS positioning accuracy issue may lead to more accurate traffic state estimation and prediction, hence resulting a substantial impact on the development strategy and policy of ITS technology, as well as on the travel experience of the road users.

1.3 Research Objectives and Scope of Work

1.3.1 Research Objectives

The research has three specific objectives:

- Quantify the relative positioning error from the position data collected via GPS-enabled smartphones using different technologies/devices
- Evaluate characteristics of GPS-enabled smartphone relative positioning error and investigate the relationships between the error and traffic related attributes
- Test the feasibility of obtaining useful traffic state information using combination of GPS-enabled smartphones and Geofence, and evaluate the performance of the settings

1.3.2 Research Scope

The field experiments conducted in this research were implemented on selected freeway, highway and urban arterials in the City of Edmonton, Alberta. Because there is no way of knowing the true location of a probe unit at a timestamp, the true positioning error is not able to be determined. This study focuses on the relative positioning error, which is the discrepancy between the location estimates obtained by GPS-enabled smartphone and the location estimated provided by a professional real-time differential GPS handset.

Since the road network and space-time diagrams are often described in two dimensions, in the application of traffic data capturing and traffic state estimation, horizontal position estimate has greater importance. Hence in this study, only the horizontal relative positioning error will be studied and focused. In

addition, since the context of this study is in the field of transportation engineering, the discussion on contributing factors to the positioning error are limited to mostly transportation related factors, and other GPS errors such as ionospheric and atmospheric errors that are more import in the field of geometrics are not discussed. Feasibility of using the Smartphone GPS and Geofence for traffic data capturing measures only focuses on the accuracy and cost, the privacy issue is not the focus.

1.4 Organization of Thesis

This research is organized as follow: Chapter 1 introduces the research background and describes the motivation, objectives and scope of the research. Chapter 2 presents a literature review of existing traffic state detection technologies and related research conducted using these technologies. Chapter 3 describes three experimental designs, data collection and result analysis on estimation of position accuracy using different technologies. This chapter also conducts regression analysis to investigate the relationship between position error and traffic related factors. Chapter 4 evaluates the feasibility of using GPS-enabled smartphones and Geofences for traffic states estimation, and discusses the performance of the Geofences by comparing the estimated values to ground truth values. Chapter 5 concludes the major findings and contributions of this research. This chapter also presents the limitations of this study, which leads to future work and recommendations for related topics.

CHAPTER 2. LITERATURE REVIEW

This chapter summarizes some of the traditional and state-of-the-art traffic-monitoring technologies. The probe technologies such as cellular network and GPS based traffic monitoring are emphasized.

2.1 Introduction

Accurate and reliable traffic information is essential at all stages of transportation planning, operation and maintenance. To cope with rapid increased population and motorization while retaining safe and efficient transportation system, many efforts have been put into researching and improving the traffic monitoring technologies to gather useful historical and real-time traffic information. The detection, estimation and prediction of these information plays important role in effective traffic monitoring. The mechanism and application of some of these traffic data collection technologies are discussed in this chapter.

2.2 Conventional traffic monitoring technology

Conventional traffic monitoring technologies use stationary sensors that provide relatively accurate information. These sensors can be intrusive and non-intrusive, where intrusive ones are often installed within or across the pavement surface and their locations are usually strategically chosen to provide coverage for major roadways. Non-intrusive detectors or sensors are installed on the roadside or attached to the traffic signposts which minimize the interruption of the traffic flow.

An example for such type of detectors would be inductive loop detectors which have been used for traffic monitoring in many decades. Inductive loop detectors are intrusive traffic detection sensors that are installed under the pavement with their wire loops powered by electronic units at certain frequencies. When vehicle presence is detected by the loop, the frequency of electronic unit will be changed to reach a certain threshold, and traffic controller device will be triggered [8]. An illustration of loop detector set up is shown in Figure 1.

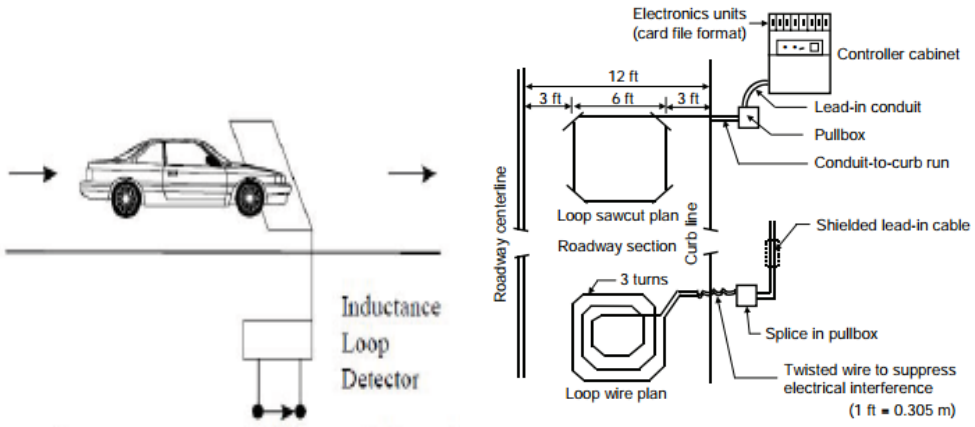

Figure 1 Inductive Loop Detector [8] [9]

These detectors are capable of providing continuous traffic volume count at fixed points, and they also outputs point-based vehicle speed estimations using single loop or loop pairs with statistical algorithm [10] [11].

An example on the non-intrusive detection technology is the infrared-based system. These sensors are often mounted to the overhead signpost to detect traffic volume and speed. Active infrared sensors use laser diodes to transmit low power infrared energy, and detection is based on reflection from vehicles back towards the sensor. Passive sensors detect energy from the energy emitted from vehicles or objects, and from the atmosphere energy reflected by vehicles. In both

types of infrared sensors, the reflected and emitted energy are converted to electrical signals to indicate detector of vehicles [8] .

The conventional intrusive detectors often impose high installation and maintenance costs, and unbalanced installation rates of these sensors in the urban and suburban regions lead to unbalanced coverage rates and uneven traffic monitoring of the road network. Therefore, it is not cost efficient to widely deploy them to provide spatially continuous traffic information over the monitored network.

2.3 Probe Technology

Probe vehicle technology is a typical application of Intelligent Transportation Systems (ITS), and it provides an innovative way to collect traffic data. It commonly involved a real-time traffic monitoring system including probe vehicles equipped with on board unit such as GPS and wireless communication devices. Some examples of using probe vehicle systems, including Automatic Vehicle Identification (AVI), Automatic Vehicle Location (AVL).

AVI system involves communication between probe vehicle with electronic tags and roadside transceivers. The vehicle is equipped with electronic transponder and a unique ID, and the antenna transceiver stations are set up in every two to five kilometers. When vehicle enters the roadside antenna's detection range, the radio signal will contain the information about timestamp and IDs for transponder and antenna, and this information will be sent to the management center by roadside units.

The AVL system has mostly been used by transit agencies for public transit planning. The position and status of the transit fleet vehicles are monitored through use of technologies such as ground-based radio navigation, and signpost-based technologies. For ground based radio navigation, traffic data is collected by communication between probe vehicles and radio towers. For signpost based technologies, the communication is between the probes vehicles with transmitters mounted on existing signpost structure [12] [13] [14].

These probe vehicle systems usually uses high-cost, on-board equipment on certain vehicles for traffic data capturing and the penetration rate are usually low [13] [14]. With emerging wireless communication applied with probe system technologies, there is an observing tend to incorporate mobile sensors to obtain real-time traffic information through estimating the device location. Different technologies such as short range tracking (infra-red, radio-frequency, Wi-Fi, etc), GPS, and cellphone network positioning system can be used [15]. The accuracies of detect device locations using these technologies varies, but in general, these new mobile sensors have the ability to acquire massive traffic data that covers wide spatial area and are economically feasible. Short range traffic detection involves propagation of a physical wave at fixed time interval. The sensors detect the moving device and pick up the wave emitted from transmitter and relay it to the detection software. The device location can be identified by inferring antenna coordinates, measuring signal strengths of access points.

2.3.1 Cellular Probe Technology

Cellular networks have become an extensive wireless communication infrastructure with global coverage. Cellular service areas are divided into hexagonally shaped districts/cells, and each of the cells has a cellular tower associated with it. With cellphone signals, a cellphone can be located using triangulation of the cell phone towers near the cell phone location. As a mobile client moves through the network, the mobile device is allocated to the cellular tower with which it is receiving the greatest field strength [14] [16].

Handoff based location solution is often used in the Global System for Mobiles (GSM) network. The handover data can be regarded as records of mobile probes' trajectories on the road network. When a mobile phone travels from one cell into another, a change of cell-ID indicating handoff is been performed. Theoretically, a handoff is considered to be located in the border of two adjacent cells in the GSM network. When the GSM network is overlapped with the road network, handoff location can be approximated to a point on the matched road link [17] [18].

Studies have shown that cellular probe technology could be applied to a coordinate-based approach and a handover-based approach to traffic monitoring. The coordinate-based approach requires the coordinates of the cellphone, which is similar to GPS probe technology. Location accuracy is the key issue for this approach. Studies performed to assess the performance of this approach include the CAPITAL (Cellular Applied to ITS Tracking and Location) project, and the US Wireless Corporation Test etc. Some researches attempted to exploit network

based solutions using handover approach, and their evaluation results revealed that they could produce promising traffic information [19] [20] [21] [22].

The cellular probe technology-based traffic data collection method has several distinct advantages, including large sample size, large spatial coverage, and high penetration rates, over other conventional methods. As of 2007, the global cellular phone penetration rate was over 50%, ranging from 30-40% in developing countries (with an annual growth rate greater than 30%) to 90-100% in developed countries [23]. However, the main drawback of cellular probe technology is that its location accuracy is comparatively lower than other technologies, such as GPS. Its location accuracy depends greatly on the density of the cellular towers. A study by Mohr et al. used three different cellular operators in the U.K. and found that the horizontal error varies greatly across urban-rural gradients. The median error was about 246 m in a dense urban area, and 626 m in a rural area [24].

The application of the cellular positioning technique has been investigated in several studies. Lots effort used cell tower signal triangulation to estimate travel time and speed information. Sanwal and Walrand studied the use of probe vehicles to collect traffic data for estimation and prediction of traffic behavior, and key issues involved in design of such system was discussed [25]. Bar-Gera examined the performance of a system based on using information from cellular phone service providers to measure traffic speeds and travel times. He compared the cellular measurements with that of dual magnetic loop detectors, and found that there is a good match between the two measurement methods, and that the

cellular phone-based system can be useful for various practical applications [26]. Yim and Cayford conducted an evaluation on the feasibility of using cellphones as traffic probes for the Bay Area Network. The study showed that accurate travel time estimates can be obtained, and assuming a 5% penetration rate, freeway link travel time estimates can achieve 95% accuracy [27].

2.3.2 GPS-Probe Technology

Overview of GPS

GPS is a satellite-based radio navigation system developed by the United States Department of Defense [28]. GPS was initially used as a military system and the operational optimal accuracies were intentionally degraded by a selective availability (SA) method, which dithered the satellite clocks and caused a range error with a standard deviation of 24 meters (m) [29]. Since the SA method was removed in May 2000, the single point accuracy of GPS has dramatically improved allowing GPS use in more applications. All users with GPS receivers are able to reach accuracy levels of approximately 18m horizontal, 28 m vertical and 100 nanoseconds [30].

GPS consists of three segments: the space segment, the control segment and the user segment. A typical configuration of GPS based probe system is demonstrated in Figure 2.

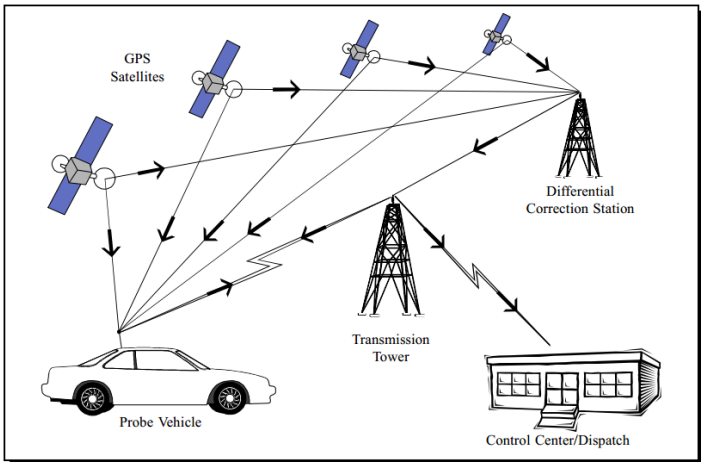

Figure 2 Configuration of GPS based probe system [9]

The space segment includes 24 satellites that broadcast navigation signals to receivers through carrier waves. The control segment monitors the location and status of the satellites that are in the space segment. The end users of the GPS receivers are the user segment. The receivers calculates the time the radio signals travel from satellites to the receiver and estimate their locations on earth by calculating travel times of signals between the satellites and GPS receivers.

GPS position accuracy varies and changes in different circumstances and is greatly affected by errors, including tropospheric delays, ionospheric delays, satellite clock and ephemeris data, orbital and atmospheric errors, and multipath. The ionosphere is the layer of the atmosphere ranging in altitude from 50 to 500 km. It consists largely of ionized particles which can exert a perturbing effect on GPS signals. The troposphere is the lower part of the earth's atmosphere that encompasses our weather. Mathematical models of the atmosphere have been research to take into account the charged particles in the ionosphere and the varying gaseous content of the troposphere.

As GPS became widely used to collect vehicle probe data, the accuracy of the data has been reviewed in different applications. Meaker and Horner proposed an Automatic Position Reporting System (APRS) that uses GPS probe vehicles to collect speed, heading, and position data. The authors compared the speed data retrieved from the probe system and traffic loop sensors, and showed that the speeds of the probes and the loop sensors were largely in concordance; however, detailed statistical analysis was not provided [31]. Schussed and Axhausen described a post processing procedure to process basic raw GPS data. The authors used the proposed procedure for trip and activity detection, and mode detection. The results were compared with the Swiss Micro-census on Travel Behavior 2005, which confirmed that the trip and activity detection works properly, the distance distributions of the individual modes derived from the GPS data were similar to the census data, and GPS has the advantage with respect to temporal and spatial accuracy [13].

GPS-Enabled Smartphone Probe

In the era of multimedia convergence, a new data collection approach is based on GPS-enabled smartphones. From 2000, cell phone providers in the United State of America and Canada have started embedding assisted GPS (AGPS) chips in their mobile devices to enhance the location based services. The AGPS enables the service providers to determine the phone locations within 15 meters. [32]. As there are an increasing number of smartphone users, and more advanced GPS chip feature is deployed, vehicle location estimation based on wirelessly transmitted sparse data via smartphones is a recent area of interest. More accurate mobile

probe data have been integrated with point detection data to estimate freeway travel times [33] [34] [35] [36]. Aguilar et.al conducted study on the position accuracy of multimodal data from GPS-enabled cellphones to fill the gap of little quantitative information about the reliability of GPS data obtained from GPS-enabled cellphones in most real-world application settings. The study result demonstrated the result of location fix attempts over different transportation modes in an urban environment, and concluded that location based transportation applications are feasible using current GPS-enabled cellphone technology. The quantitative data presented in the paper focuses on the percentage of GPS fixes obtained by each mode and the analysis results indicated little significant differences in the number of valid GPS fixes obtained from users [37]. A field experiment was conducted by Yim and Cayford in 2001 [38] to compare the performance of cellphones and GPS devices for traffic monitoring. The study concluded that the GPS positioning technique is more accurate than cellular tower positioning. If GPS-equipped cellphones are widely used, then they will become an attractive and realistic alternative for traffic monitoring.

2.3.3 Concept of Geofence

A Geofence is a virtual boundary created around a physical geographic space. Each Geofence defines an area with a set of coordinates at vertices, and its establishment and maintenance are undertaken by a range of GPS-enabled devices including computers, smartphones, and handheld GPS receiver etc. The Geofence can be created to cover varies shapes and sizes of an area, and a unique ID will be assigned to Geofence. When a GPS-enabled smartphone crosses the boundary to

enter the predefined Geofence, a location update for that smartphone will be triggered, and the location information of that smartphone along with the triggered Geofence ID will be sent to the traffic monitoring server. As a vehicle traverses the Geofence, its location update comprised of timestamp, Geofence ID, the direction of crossing, location coordinates, and device ID will be sent via wireless network to the server.

Compared to physical traffic sensors, Geofences are more flexible, such that they can be deployed at various locations and with different shapes regardless of construction and incremental cost. The deployment does not interfere with traffic nor construction work which minimizes the interruption to the traffic flow and user cost. After setting a Geofence, it is also easy to adjust and change with minimal cost.

2.4 Summary of Literature Review and Research Implications

Studies on the conventional and probe data collection methods have showed that conventional sensors are site specific and their installation and maintenance cost are quite high. Any adjustment made to these detectors may require closure of a traffic lane or may interrupt traffic flow and induce extra user costs. In the cases when there are defects in some of the sensors, large amount of measurements may be missing. The probe vehicle technologies are not infrastructure related and the spatial coverage is not captive. However, traditional probe vehicles with on board equipment may be costly and the penetration rate is low which limits the systematic implementation. In addition, although the cellular

network positioning technique may have higher penetration rate than other probe technologies, the accuracy of location estimates may not be enough. Since some of the probe devices are monitored regardless with the user's situation, there is increased concern on user privacy and public policy.

Existing studies on each of the aforementioned positioning techniques and devices focused on their deployment algorithms and performances on a specific transportation application, such as travel time estimation, collision warning and freight management. Although there was some discussion on the cellphone and GPS positioning error, the context was mostly limited to freeways due to the advantages of working with a controlled access environment. The magnitude and characteristics of such error are not discussed in detail. A systematic comparative study has not been carried out to quantify the accuracy of the position estimates using different technique, and the impact of some transportation related factor on the positioning error is not exploited. This study intends to fill this gap so the most suitable devices can be selected for traffic data collection and management purposes.

This study focuses on investigating and comparing the magnitude and characteristics of the relative positioning error from different devices as well as evaluating feasibility for their application on City of Edmonton roadway network.

CHAPTER 3. SMARTPHONE GPS POSITIONING ACCURACY AND ERROR CHARACTERISTICS

This chapter describes the details of the experimental design and presents the result of the field tests conducted on several roadways in City of Edmonton. The magnitude and characteristics of relative positioning error is described, and some contributing factors are analyzed by regression analysis.

3.1 Introduction

An experiment was conducted to meet the fundamental goal of estimating and evaluating the relative GPS positioning error from four technologies and devices including professional handheld GPS device Juno, cellular positioning, smartphone GPS, and Geofence.

The objectives of this experiment are:

- To estimate the relative positioning error among several data sources
- To evaluate the characteristics of the error and relate it to transportation related factors
- To evaluate the relationship between some of these factors and the relative position error.

3.2 Experimental Design

To estimate the relative GPS positioning error among several data sources, three scenarios are set up:

- Scenario 1 - Estimate relative GPS positioning error of the GPS-enabled smartphones with comparison to the output from the professional GPS handset Juno.
- Scenario 2 - Estimate relative positioning error of using the cellular network or by comparing the estimated handover points in each trial to the estimated coordinates of the true handover locations.
- Scenario 3 - Estimate the positioning error of using GPS-enabled smartphone and Geofence with comparison to the output from the Juno and the location of Geofence, as the ground truth.

3.2.1 Study Site

This experiment was conducted on various days between June 11th, 2013 and April 30, 2014 on various roadway segments including freeway, highway and arterial in City of Edmonton.

The freeway segment is mainly along a section of Whitemud Drive, which is a multilane urban freeway with most sections in the east-west direction and one section crossing the North Saskatchewan River goes in the north-south direction. The section of Whitemud Drive traversed during the experiment is between its intersection with 170 Street and 75 Street.

Highway segment includes a section of Anthony Henday Drive and Queen Elizabeth Highway. Anthony Henday Drive is a multilane ring road around the

City of Edmonton, and is numbered Highway 216 in the provincial highway system. The section of this highway traversed during the experiments was from its intersection with Whitemud Drive to the directional interchange with Queen Elizabeth Highway. The speed limit on Anthony Henday ring road is 100 km/h. Anthony Henday Drive and Whitemud Drive are both included in the first connected vehicle test bed in Canada. Since the connected vehicle may use advanced wireless communications, GPS, smartphone based probe technologies and smart infrastructures to allow wireless communication among vehicles and infrastructures to share their locations and information, the study on positioning error of GPS-enabled smartphones along this section of test bed may help accomplishing the goal.

A section of Queen Elizabeth Highway was also included in the experiment. This section of primary highway starts from its connection with south Anthony Henday to its intersection with Highway 625 near the Edmonton airport area. The speed limits are 90 km/h near the boundary of City of Edmonton and 110 km/h beyond the city boundary to further south.

The urban arterials traversed during the experiment include several streets in the north-south direction, and avenues in the east-west direction. Figure 3 below shows the coverage of the collected data on corridors included in the experiment. The roads in pink color are the highways, and in blue is Whitemud Drive, and the roads in green are various urban arterials.

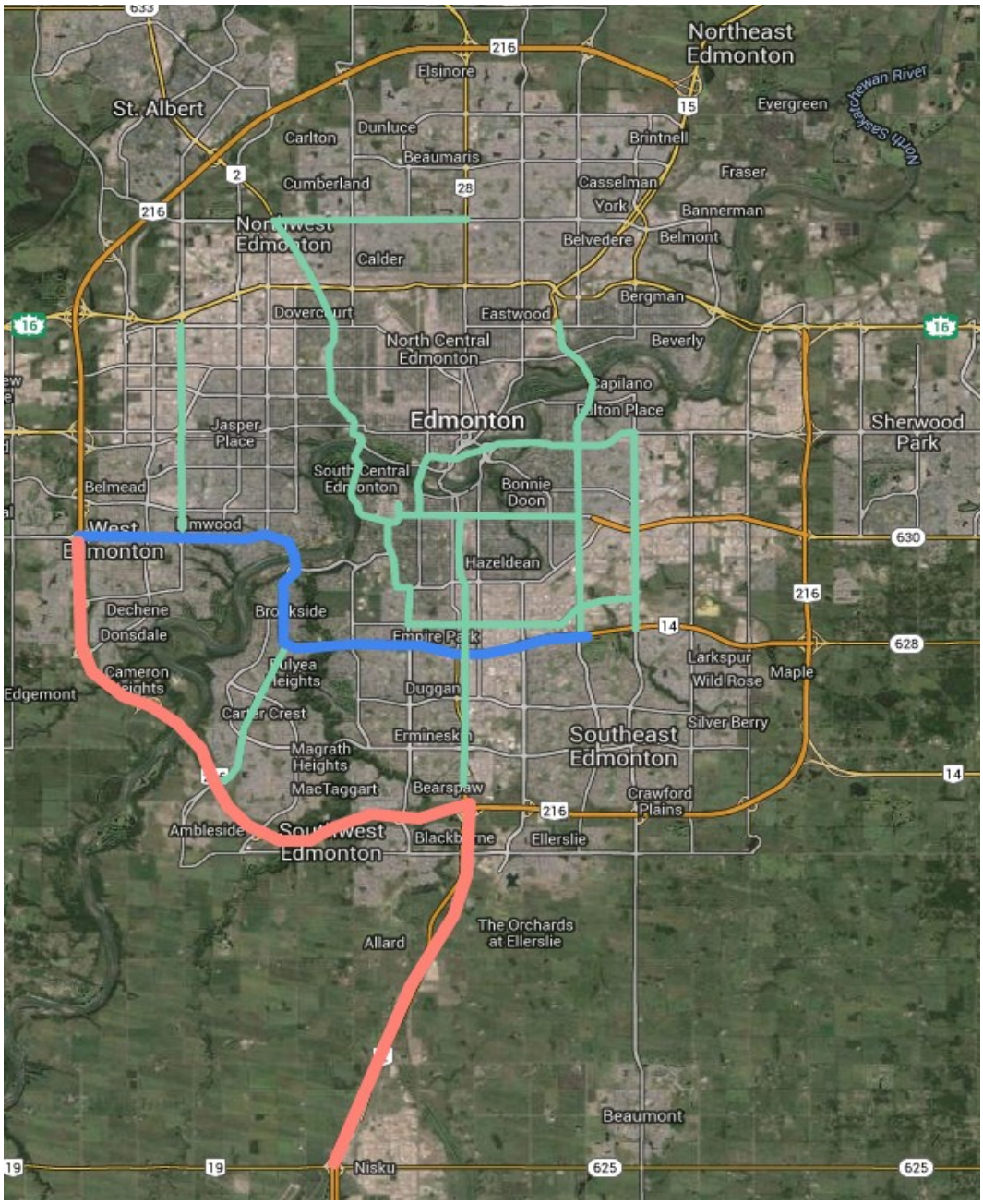

Figure 3 Study Corridors

3.2.2 Equipment

The equipment used in this experiment includes a passenger vehicle equipped with handheld professional GPS receivers, GPS-enabled smartphones and video camera.

The professional handheld GPS receivers used is a product from Trimble, a leading provider of advanced location-based solutions that integrates its positioning expertise in GPS, laser, optical and inertial technologies with application software, wireless communications, and services. This handheld device named Juno is empowered with a fully integrated, GPS-based data collection system. This device includes a high-sensitivity GPS/SBAS (Satellite-Based Augmentation System) receiver and an antenna and has 12 channels with L1 frequency coding. The update rate is 1 Hz and the time to first fix is typically 30 seconds. Juno operates with the GNSS TerraSync field software and records coordinates with a time interval of one second. After differential correction, with real-time SBAS, the Horizontal Root Mean Squared (HRMS) accuracy can reach 2-5 meters. The HRMS accuracy can be increased to 1-3 meters with code post-processing empowered by Trimble DeltaPhase technology supported in the Trimble GPS Pathfinder Office software [39].

There were several GPS-enabled smartphones used in the data collection including models using Android and IOS platforms. Three smartphone applications with GPS tracking and logging functions were used as tools to record and save coordinates of the traversed path. The settings of the applications were adjusted so that the GPS position data would be recorded at one second intervals. In all the equipment, the position datum was set to World Geodetic System 1984.

3.2.3 Error for different data sources

Position information including timestamp, latitude, and longitude at every one second is collected by the GPS-enabled equipment. This data is referred as

trajectory data since vehicle trajectories can be reconstructed from it. Trajectory data was processed after the experiment to conduct more detailed analysis on data quality and characteristics. The relative positioning error is measured using the following technologies/devices:

- Professional GPS handset
- GPS-enabled smartphone
- Cellular network positioning
- GPS-enabled smartphone with Geofence

3.2.3.1 Scenario 1: Smartphone GPS VS. GPS handset

A preliminary test was conducted first to ensure the feasibility of the field test. The experimental procedure used in the preliminary test was then carried out to collect more data in the field test. The test route was traversed three times along Whitemud Drive with a passenger car. The data set from GPS handset and the smartphone applications include location information such as latitude, longitude, altitude, timestamp, etc. The position data collected by GPS handset is first imported to the Pathfinder software for post-processing and transformed to northing and easting units; the processed data are then exported to Microsoft Excel for calculation and analysis. The location data from smartphones are exported from the applications to Excel spreadsheets. Both sources of data can be mapped to Google Earth for comparison.

For position error estimation, the GPS position data from the devices was compared at each second. Since the Juno handset from Trimble is a professional surveying tool that provides accuracy to meet high expectations (1-3 m range

accuracy), the GPS data from the Juno handset was considered as the ground truth in this experiment, and the discrepancy between the GPS data from Juno and the other devices are considered the relative positioning error. The differences between the location data collected using smartphone GPS and Juno are referred to as the easting relative error, northing relative error and relative horizontal error.

The easting refers to eastward distance measured from horizontal datum in meters; hence, the relative error in the easting direction is the differences in the easting measures from the two data sets. Similarly, the northing error refers to the differences in measurements in the northward direction. To obtain the horizontal distance, we used great circle distance concept which is the shortest distance between the two known locations with latitudes and longitudes over earth's surface.

A great circle is a section of a sphere that contains a diameter of the sphere (Sections of the sphere that do not contain a diameter are called small circles. A great circle becomes a straight line in a gnomonic projection [40] [41]. In mathematics and cartography, a great circle distance is the shortest path between two points on the surface of a sphere. All lines of longitude are great circles, while the equator is the only latitudinal great circle.

A great circle distance is calculated by finding the interior spherical angle between the two points and then multiplying that angle by the radius of the earth. The interior spherical angle multiplied by the radius of earth yields the great circle distance between two locations. This formula is known as the Haversine Formula [42] [43].

$$\Delta\sigma = 2\arcsin\left(\sqrt{\sin^2(\frac{\Delta\phi}{2}) + \cos\phi_s \cos\phi_f \sin^2(\frac{\Delta\lambda}{2})}\right)$$

$$d = R \times \Delta\sigma$$

Where $\Delta\sigma$ is the interior spherical angle,

$\Delta\phi$ is latitude 1-latitude 2

ϕ_s is Latitude 1

ϕ_f is Latitude 2

$\Delta\lambda$ is longitude 1 – longitude 2

d is the distance between the two points

R is the earth's mean radius =6,371km

When converting the latitude and longitude measurements to easting and northing values in UTM 12 system, there exist some error in the transformation process; this error may contribute to the overall positioning error estimation for all devices. Since we are estimating the relative positioning error among devices, this error is left in as a contributing factor in the overall estimation throughout the study.

3.2.3.2 Scenario 2 : Positioning Error from Cellular Positioning

For this scenario, the GPS data was collected by GPS handset, and cellular positioning data was collected by a smartphone. But in this case, another application was installed on the Android platform to collect the cell-IDs for cellular positioning purpose. In the cellular location logging data, each recorded coordinates with latitude and longitude was estimated through cell towers, and a corresponding distinct cell-ID was also recorded. The cellular data including the

timestamp, latitude, longitude and cell-IDs can be exported from the application as a comma separated values (.csv) file, then exported to excel for analysis and imported to ARCGIS software for trajectory mapping and color coding. The location accuracy at each timestamp was first analyzed in the similar fashion discussed in the previous section, and then a handover based location accuracy evaluation was carried out.

As the vehicle travels along the test route, it receives signals from different cell towers, and the cell-ID changes accordingly. The point where a change of cell-ID is observed is considered the handover point. Because radio signal propagation will be influenced by reflection, refraction, diffraction and other influencing factor, the handover location will never be a fixed point; instead, it will fluctuate in a short length over the matched road network. Each time a change of cell-ID is observed, a handover location can be approximated, and an estimated true handover location is calculated by averaging the approximated handover locations in different trials. The deviation between the observed handover locations and estimated true handover locations are calculated to be the discrepancy and will reflect the location accuracy.

3.2.3.3 Scenario 3 : GPS-Enabled Smartphone and Geofence

This scenario involves the use of Geofence concept. Before the experiment, a set of Geofences were defined to be in rectangular shape, each consists of four GPS coordinates. These shapes are mapped onto short sections of roadways. The coordinates are downloaded into the smartphones and as the vehicle carrying the smartphones enters a Geofence, the Geofence will be triggered, and the position

update is sent to the Geofence system server. A total of 99 Geofences were deployed on three roadways covering both travel directions. Forty-three of them were deployed along Whitemud Drive, 19 were along 170 street and 34 were along 75 Street (Geofence locations are shown in Figure 4). This part of the experiment also requires the use of GPS-enabled smartphones, which support the execution of an application that can log GPS information, download and cache Geofences from the server to detect fence traversal. Video camera mounted to the vehicle window is also used. The video data provides accurate timestamp of entering the Geofences and the exact travel time in each segment.

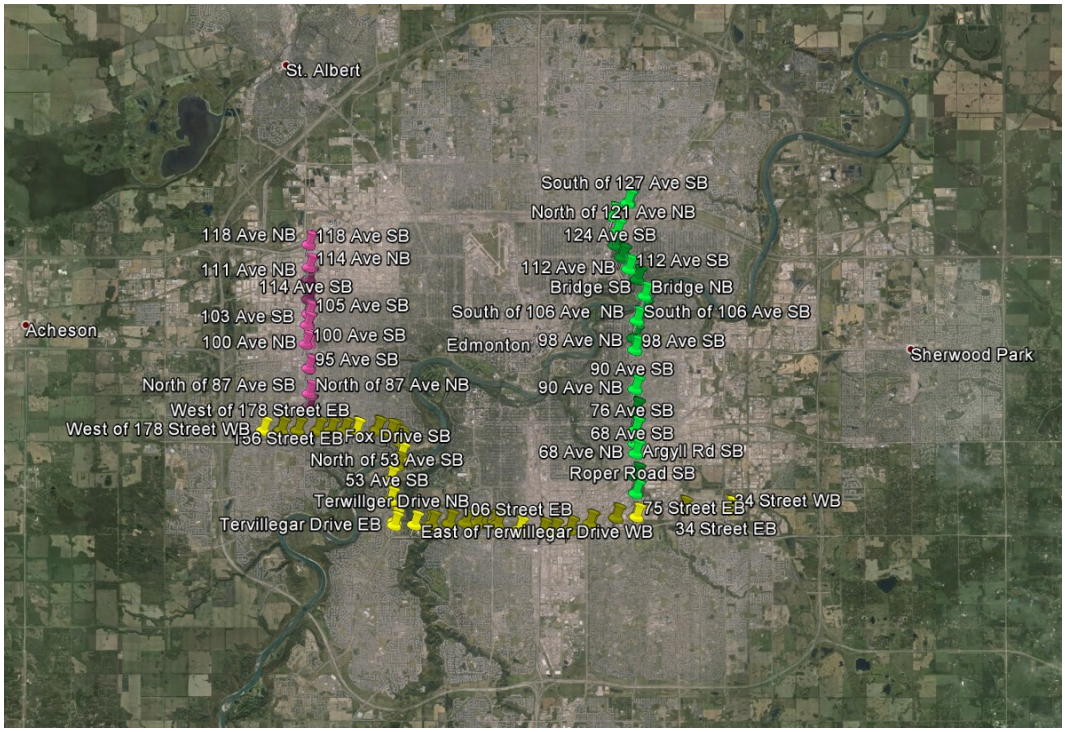

Figure 4 Geofence deployment in City of Edmonton

The mechanism of this part of the experiment is explained in Figure 5 As the vehicle traverses the test segment, the GPS-enabled smartphones run an application called Drivewyze, which will allow location information to be collected from the devices when the vehicle travels in the Geofence. A Drivewyze

display will appear on the smartphone screen indicating entrance into the Geofence, and the location points collected within the Geofence will be sent to the server. Simultaneously, the same timestamp, at which the Drivewyze notification appeared on the smartphone, will be recorded by the video camera, indicating reception of first data point after the vehicle enters the Geofence. In addition, the coordinates from the Juno handset output is also considered as a location reference used to compare with the position and timestamp log files stored locally on the phones. The server receives the location information including the device ID, event time, Geofence number, latitude, longitude, carrier, phone type and version of the application and stores the data for further calculation.

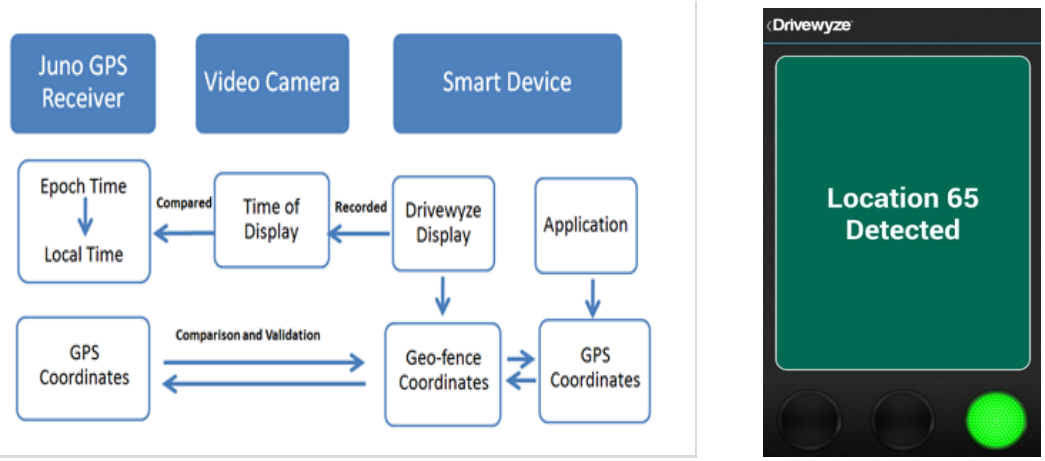

Figure 5 Experimental Design for Scenario 3

A preliminary test was set up to first test out the operation of the Geofence, and then a more comprehensive test was conducted to collect more Geofence data. Six different smartphones with Drivewyze application were used to collect location information when driving along the test route.

3.3 Experimental Results

This section presents the results for three scenarios from the experiments and discusses the findings and implication.

3.3.1 Result for Scenario 1- Smartphone GPS compare to Juno

3.3.1.1 Preliminary Test

This section analyzes the quality of the data collected and stored in the smartphone and its relative accuracy comparing to professional GPS handset. For the preliminary test, the data collection was repeated three times along Whitemud Drive (Trial 1, 2 and 3 respectively). Both the smartphone GPS data and the Juno data can be output to a .kml file, and the vehicle trajectory can be obtained by projecting to Google Earth. The smartphone data points in the preliminary test were collected by using three applications on the Android platform. The descriptive statistics for the GPS data outputs from the equipment were presented in Table 1.

Table 1 GPS Position Comparison between Smartphone and Handset Output

Application	Application 1			Application 2			Application 3		
Trial	1	2	3	1	2	3	1	2	3
Mean	4.59	2.60	2.79	5.37	2.49	2.95	4.63	2.90	2.44
Standard Deviation	1.89	1.26	1.34	2.42	1.22	1.52	1.73	1.56	1.24

As shown in Table 1 the average GPS positioning error of the GPS-enabled smartphones varies slightly among applications. For trial1, the average error is between 4-5.5 m, and the error data ranges between 0.34-15.88 m. For trial 2 and trial 3, the average error is between 2-3 m, and ranges from 0.27-7.35m.

When projecting the vehicle trajectory to Google Earth, most of the data are placed in the middle of the driving lane, and the data constructs smooth path. Further analysis shows although there are some data points projected to the edge of the road or very close to the median of the roads, approximately 92% of the data points are correctly positioned on the roadway segments, and on average, the coverage of the collected data points is 36 points per kilometer Figure 6 shows a close up view of the projected vehicle trajectory. In (a), all of the data points are positioned to the middle lane of the freeway, and in (b), one data point was incorrectly positioned on to the median.

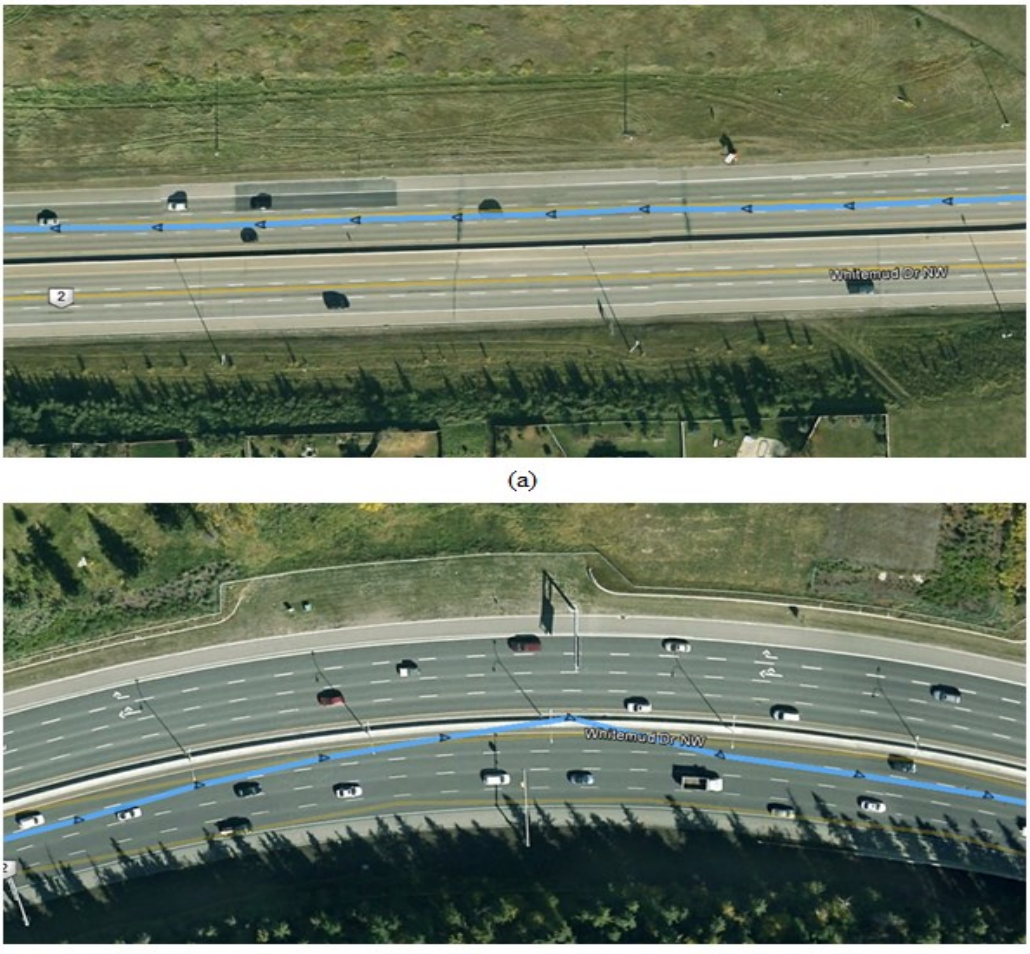

Figure 6 Vehicle trajectory projected to Google Earth

The positioning errors from the GPS-enabled smartphones are plotted with time in Figure 7. In all three trials, the application1 lost GPS signal for a short period of time, which explains why the data points from application 1 are the least compelling among the three applications. The trend of the error points are not obvious, but showing some traces of a trend of up and down movement with a peak to peak amplitude of 6 m.

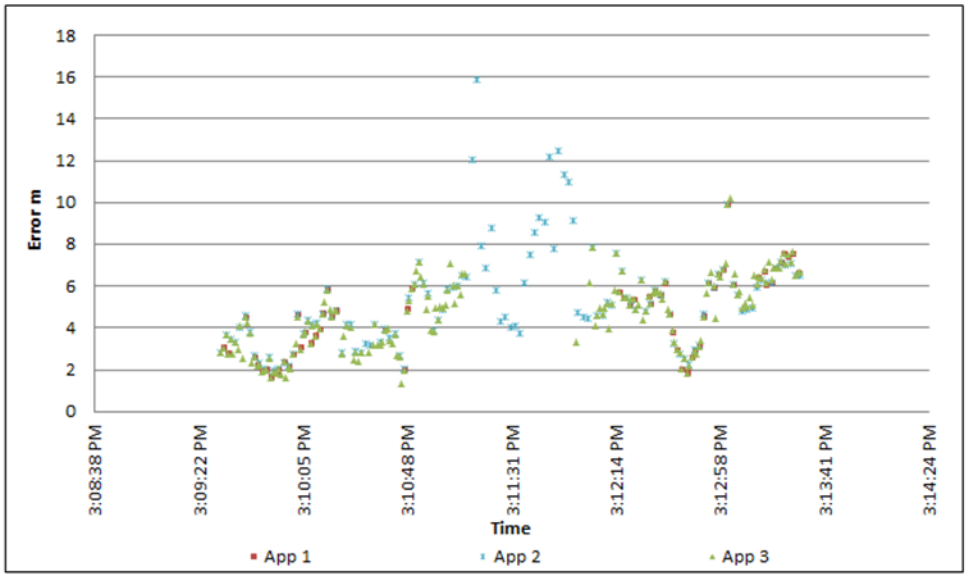

(a)

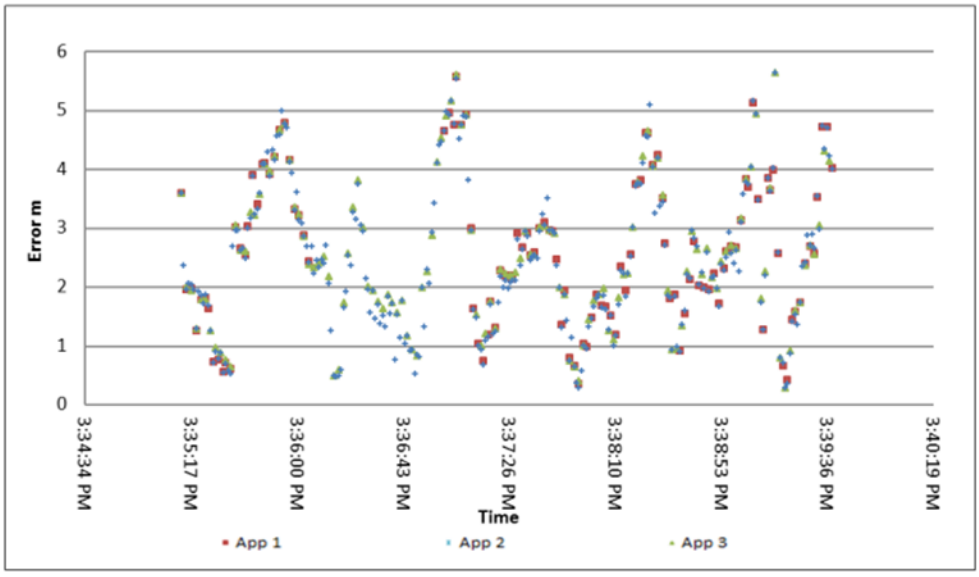

(b)

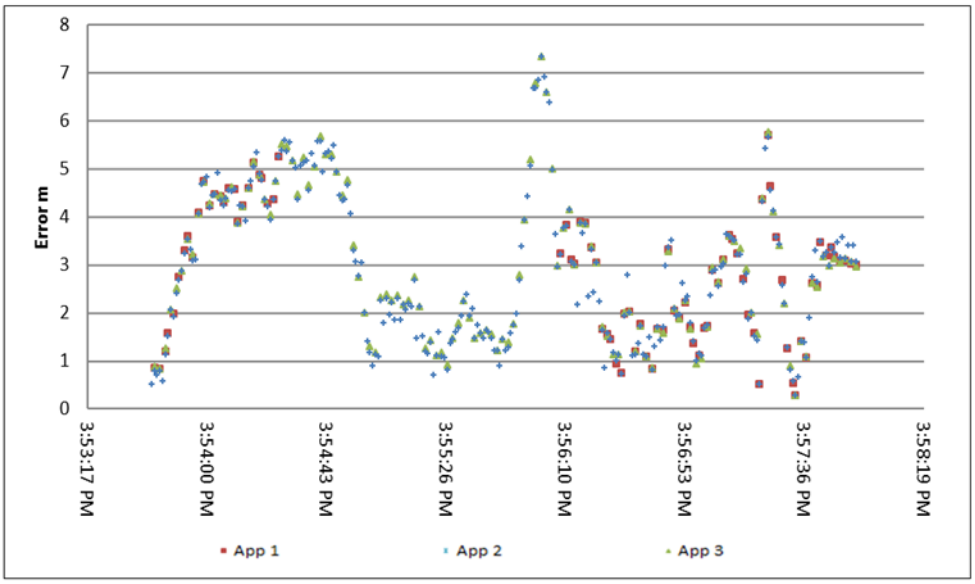

(c)

Figure 7 GPS Error Plot with Time for (a) Trial 1, (b) Trial 2, and (c) Trial 3

In the second trial , data was missing on the 1km segment of WMD from the west of 159 street to the east of 159 street. So the coverage rate for this trial is the lowest among the three. Figure 8 shows the GPS error frequency distribution and cumulative% curve. The frequency distributions for all trials are similar to bimodal. For trial1, the frequency distribution is symmetrical, and an error of approximately 6 m is the most frequent. For trial 2 and 3, the most frequent error is in the range of 2 to 3 m. From the cumulative % curve, for trial 2 and 3, nearly 90% of the smartphone data is less than 5 m, indicating good quality of the smartphone data and the feasibility of continuing this set up for more data collection and comprehensive analysis.

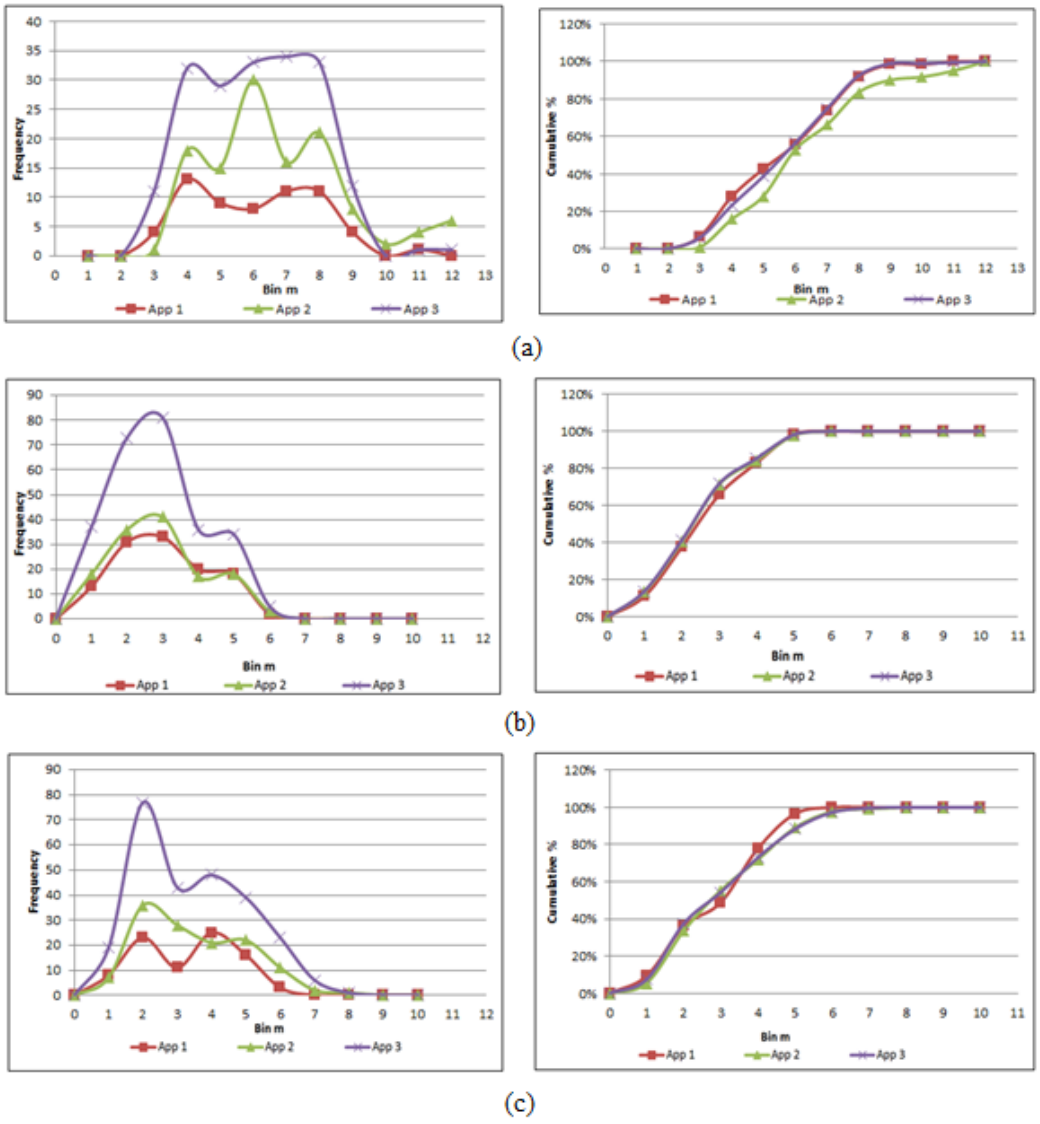

Figure 8 GPS Error Frequency Distribution and Cumulative% Curve with (a) for Trial1, (b) for Trial 2, and (c) for Trial 3

To test whether different applications on Android smartphones would yield significant differences in the sample mean, the GPS log data obtained by the four applications using GPS-enabled smartphones are compared using analysis of variance (ANOVA) test. The null hypothesis is that all means are equal, and there is no significant difference of means. The F test is used to assess whether any of the application performs on average superior or inferior to the others versus the

null hypothesis that the group means are equal; that is, all four applications yield similar mean error.

Table 2 ANOVA F test on Smartphone Application Outputs

	SS	*df*	*MS*	*F*	*P-value*	*F crit*
Trial 1	46.63886	2	23.31943	5.802285	0.003309	3.020661
Trial 2	1.999387	2	0.999694	0.648251	0.52339	3.013398
Trial 3	1.125178	2	0.562589	0.248397	0.780154	3.015157

As presented in Table 2 trial 1 data yields F critical=3.02 and F=5.80>F critical. The test obtains a large F value (greater than F critical) and a small p-value (<0.05). Therefore, at a confidence level of 95%, the null hypothesis that all group means are equal can be rejected, which means that there may be significant difference among the means of the GPS position errors obtained using the smartphone applications. Therefore, the alternative hypothesis stating the group means are not equal may be true. However, for trial 2 and 3, the F value is less than the F critical, and the P-value is greater than 0.1; therefore, since all means are equal, the null hypothesis cannot be rejected.

The reason that ANOVA test for trial 1 is significantly different from the other two may be that a part of the smartphone data in trial 1 is missing, and smartphone applications failed to provide continuous data logs throughout the experiment, which explains that the data count for application 1 is the least among the three. As none of the applications have developed algorithms to post-process

the GPS data, the position accuracy should depend on the GPS receiver in the smartphone regardless of the type of applications used.

3.3.1.2 Integrated Results

The relative discrepancy between the smartphone GPS position data and GPS handset data was calculated for all the data points collected on various roadways and on various days. A general plot of error is shown on the left in Figure 9, and horizontal dilution of precision (HDOP) is plotted on the right.

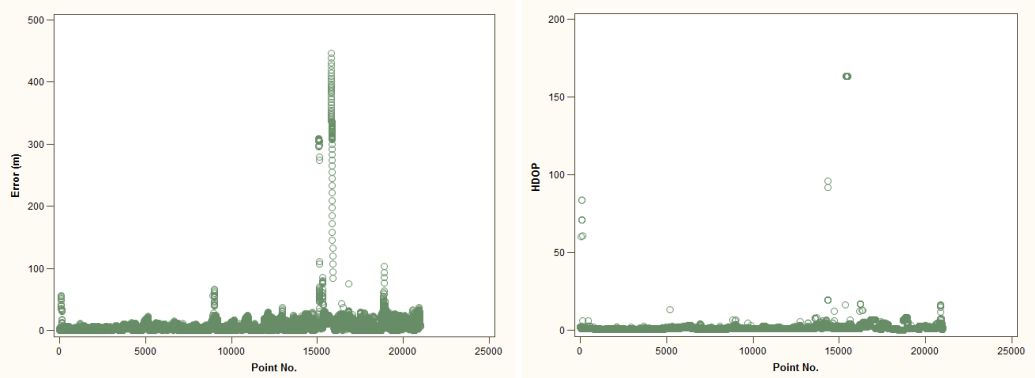

Figure 9 Plot of relative position error and plot of HDOP

Although the relative position error varies from point to point, most of the error is less than 50 m. It is obvious that error increases to a higher value near point number 0, 9000, 15000, and 19000. This stretches the range of error from 0-50 m to 0-500 m. In order to find the reason for such substantial difference in error, HDOP value was also plotted. The HDOP value is high near the same data points where the error values are substantially higher in the error plot; the large error was mostly likely correspond to high value of HDOP, which implies that the geometry of the satellites is poor at the timestamp where error is large.

The general descriptive statistics for all the GPS positioning error and for the errors that are less than 50 m are presented in Table 3 below. The 95%

confidence interval of the measurement error is computed as ±1.96 times the standard deviation.

Table 3 Descriptive statistics for smartphone relative positioning error

Mean	Std Dev	Lower Quartile	median	Upper Quartile	Lower 95% CL	Upper 95% CL
All position points						
8.99	23.69	2.75	4.84	10.01	8.67	9.31
Filtered position points						
7.32	6.47	2.81	4.88	9.93	7.23	7.41
Easting position points						
0.89	249.88	-2.69	0	3.09	-2.49	4.28
Northing position points						
-0.88	370.90	-4.61	-0.75	2.58	-5.91	4.15

After filter out the outlier points that have large errors, the mean and standard deviation value reduces. Mean positioning error for easting and northing direction are both within ±1 m. The horizontal relative error is less than 10 m. The distribution of the relative error for both filtered and unfiltered cases are presented in Figure 10. For both error distributions, the plot is lopsided to the right representing a positively skewed distribution and a greater concentration of mass to the left. The histogram plot and box and whisker plots for easting and northing error is also plotted, and both of the distribution is steeply centered on the mean.

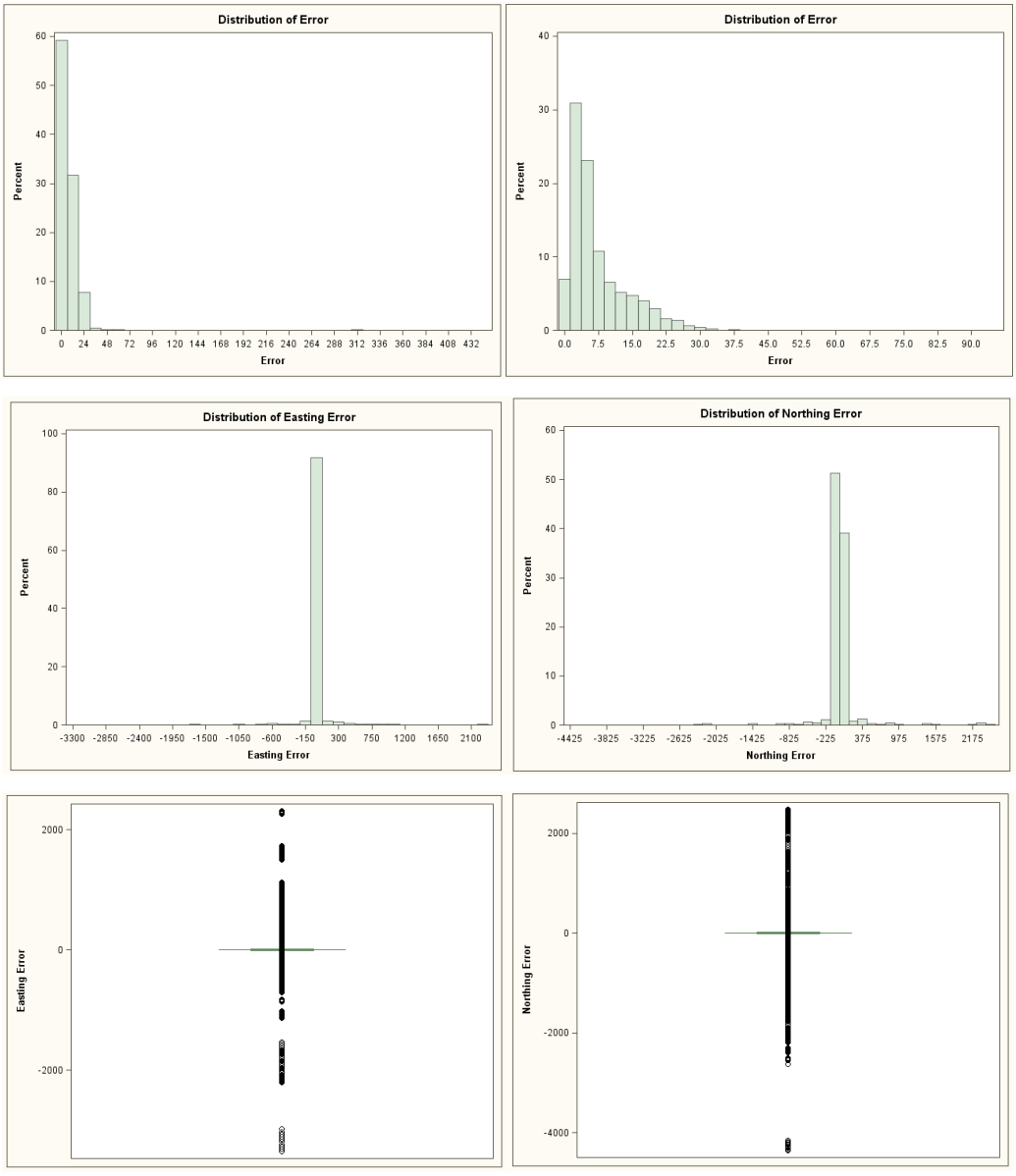

Figure 10 Distribution of relative positioning error

Probability-Probability plots are constructed using theoretical cumulative distribution function of normal, log-normal, exponential, weibull, and Gamma models to determine how well these theoretical distributions fits to the observed data. The plot will be approximately linear if the specified theoretical distribution is the correct model. Comparing the P-P plots in Figure 11, the fifth plot shows lognormal distribution with shape factor 0.84 and scale factor 1.68 fits the best to

the observed relative error data. The distribution is positively skewed, and the last plot shows the natural logarithm of relative position error is normally distributed.

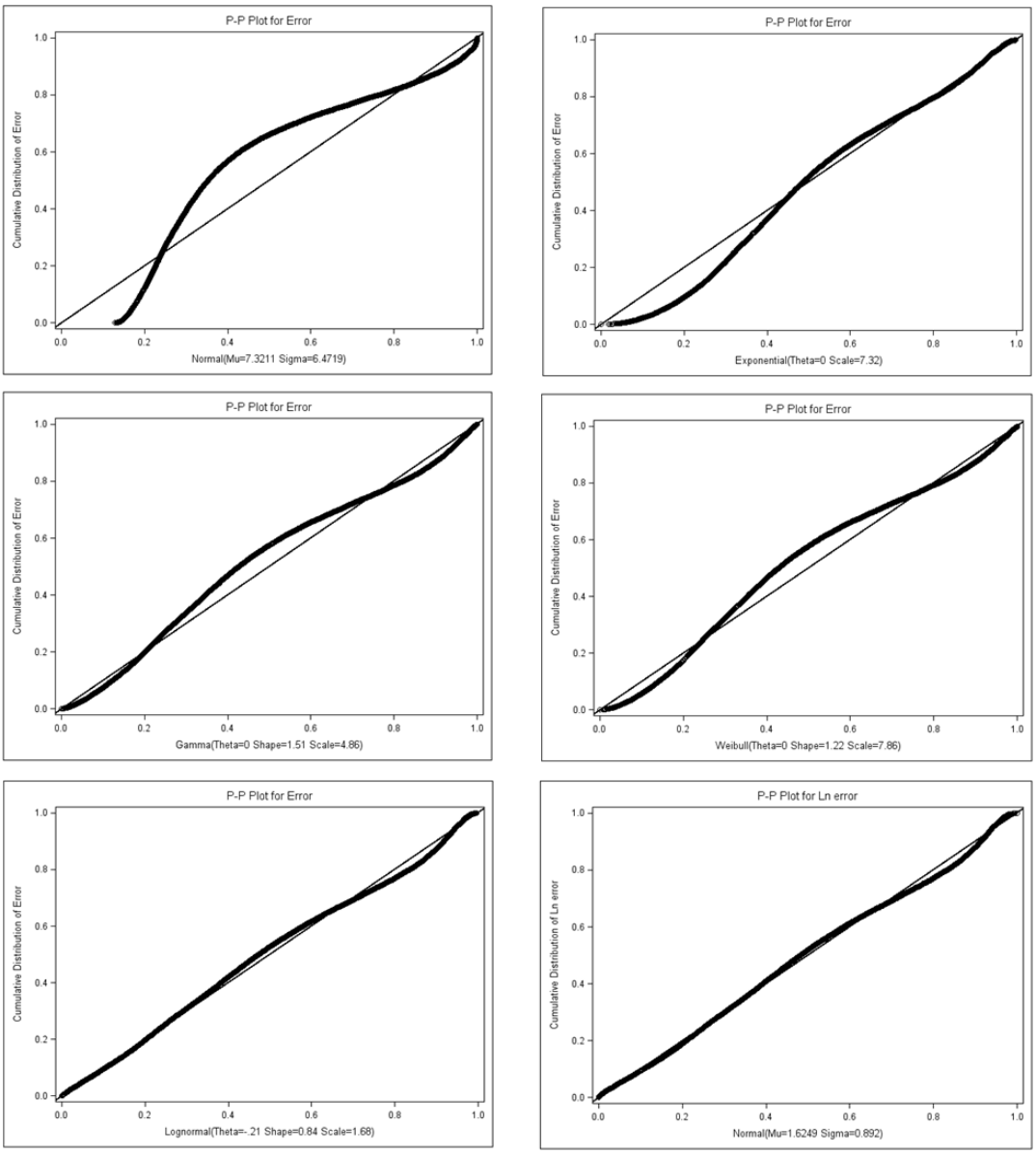

Figure 11 Fitting the distribution of the relative position error

The error data are then sorted according to type of facility, type of mode, type of view to satellite to investigate whether there are any relationships in between. Table 4 presents descriptive statistics for the relative GPS positioning

error using different facilities. The histogram and box plots for different errors are plotted in Figure 12.

Table 4 Descriptive Statistics of relative errors

	Mean	Std Dev	Lower Quartile	Median	Upper Quartile	95% CL for mean	
Free flow							
	4.35	3.71	2.08	3.25	5.42	4.26	4.43
Arterial							
	9.59	8.22	3.82	6.95	14.05	9.44	9.74
Car							
	6.71	6.59	2.65	4.43	8.26	6.61	6.81
Bus							
	10.87	8.59	4.59	9.54	15.49	10.57	11.17
Limited sight							
	10.63	10.58	3.87	8.06	14.06	10.10	11.15
Partial sight							
	9.63	8.26	3.47	6.89	14.73	9.44	9.82
Full sight							
	5.58	5.04	2.47	4.00	6.70	5.49	5.68
With mobile network							
	6.30	6.20	2.57	4.26	7.52	6.20	6.40
No mobile network							
	10.78	8.75	4.12	9.37	15.77	10.5	11.02

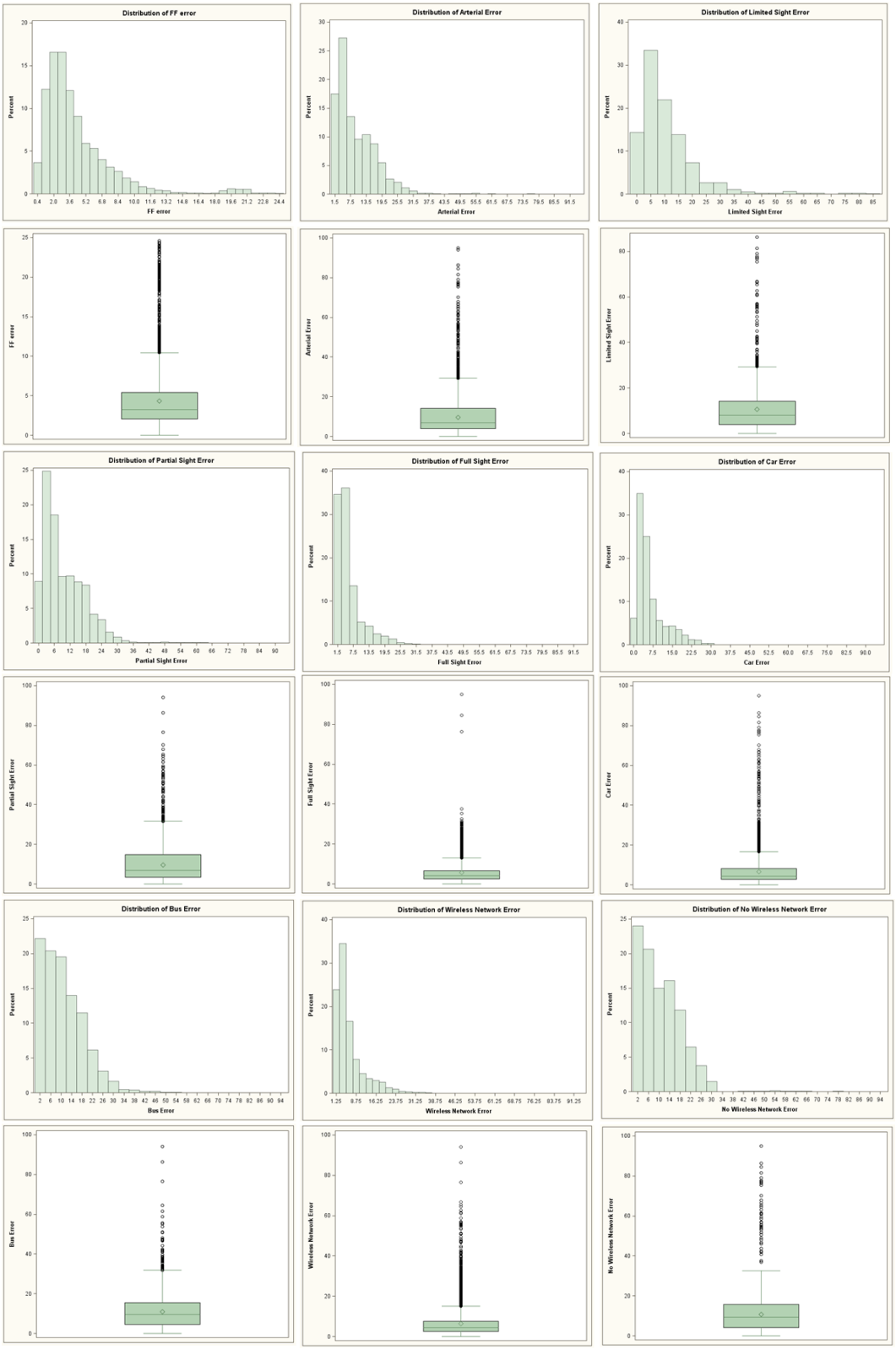

Figure 12 Plot of error distributions under different conditions

Comparison between the mean of the relative position errors and between the statistical plots for different groups shows that position error on facilities with free flow conditions are lower than that on arterials with stop and go conditions. Position points collected with limited sight to the satellite has higher error than that collected under partially open sky, and the position error for the locations with open sky and direct sight to the satellite is the least among the three. The position points collected on a car has lower error compare to that collected on the bus. Data collected with mobile network connection has lower error compare to the data collected with mobile network turned off. All histogram plots are skewed to the left of the x-axis. The plots showing larger position errors have wider distribution and longer tails.

In general, the GPS position data collected using GPS-enabled smartphones has the 95% confidence interval of the measurement error in the range of 1 to 10 m, and is considerably accurate in comparison to the professional GPS handset. GPS-enabled smartphones are capable of providing the general public with accurate and low cost location and navigation services.

3.3.2 Result for Scenario 2 : Positioning Error from Cellular Positioning

Smartphone application which uses cellular positioning technology was set to collect position data at an interval of every one second. Smartphone position data points were compared to the position data collected via GPS handset and the relative error on the easting and northing directions are analyzed and the easting, northing and horizontal errors are plotted with cell ID after removing the outliers in Figure 13.

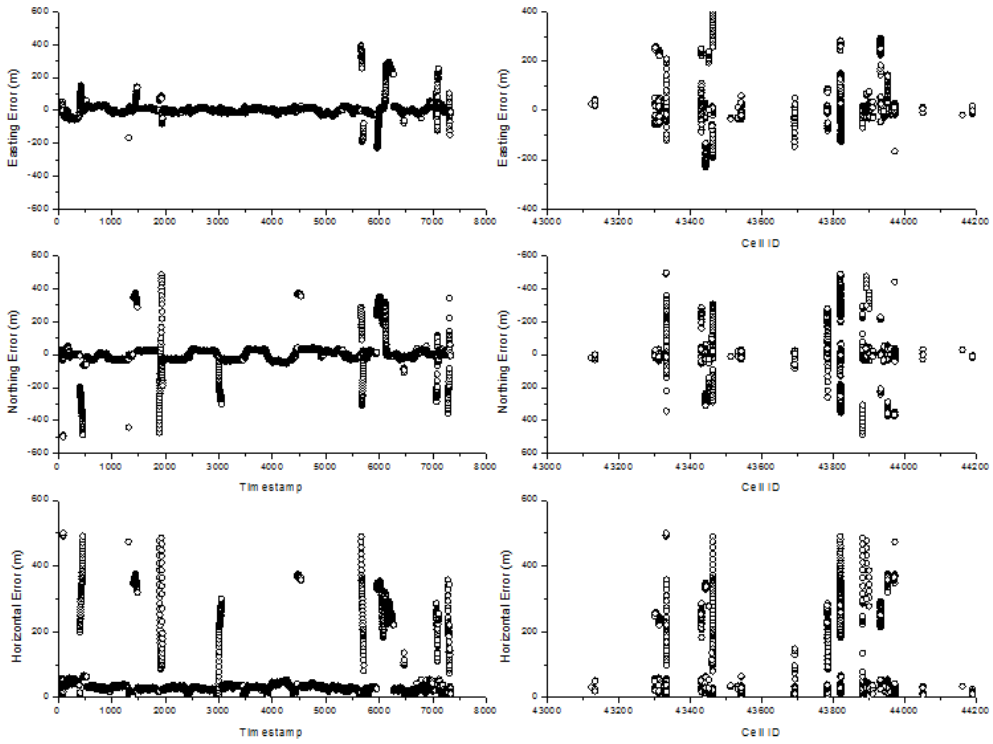

Figure 13 Plot of cellular positioning error with time and with cell-ID

The three plots on the left side presents the easting, northing and horizontal errors plotted with timestamps. The easting and northing error plots show the relative error fluctuates above and below 0 with time and the trend is more obvious in the northing error plot. The data points between timestamp 1000 to 4500 are collected while travelling along QEII outside of city boundary in the southbound and northbound directions for several trials, and the variation in position error is reflected from the repeating trend in the northing error plot. The magnitude of error reduced several times during timestamp 1000 to 4500. The magnitude of error increases when vehicle drives southbound out of the city and it decreases as vehicle drives northbound back to the city. One reason behind this variation may be that there are more cell towers within the city and fewer of them outside of city. So the cellular positioning error depends on the deployment of cell

towers. The three plots on the right shows the positioning error plotted with cell-ID. The positioning error corresponding to different cell-ID varies in a bigger range. For some cell-IDs, the corresponding positioning error varies between 0 m to 200 m, and for some other cell-IDs, the positioning error are below 50 m.

Figure 14 illustrates the distribution of the easting, northing and horizontal position error from the position data. The top three plots reflects the whole data set with outliers, the bottom three plots reflects the data after cleaning. The statistical analysis beyond this point will reflect the cleaned data set. The histograms have high kurtosis where there is a distinct peak near the mean, showing high percentage of the errors are concentrated near the mean value, and the peak declines rapidly as the values spread out to the tails. For both cases, 95% of the relative error is within ±50 m. The distribution plot of the horizontal error is skewed to the left representing a large percentage of the horizontal error is in the range of 0 to 60 m.

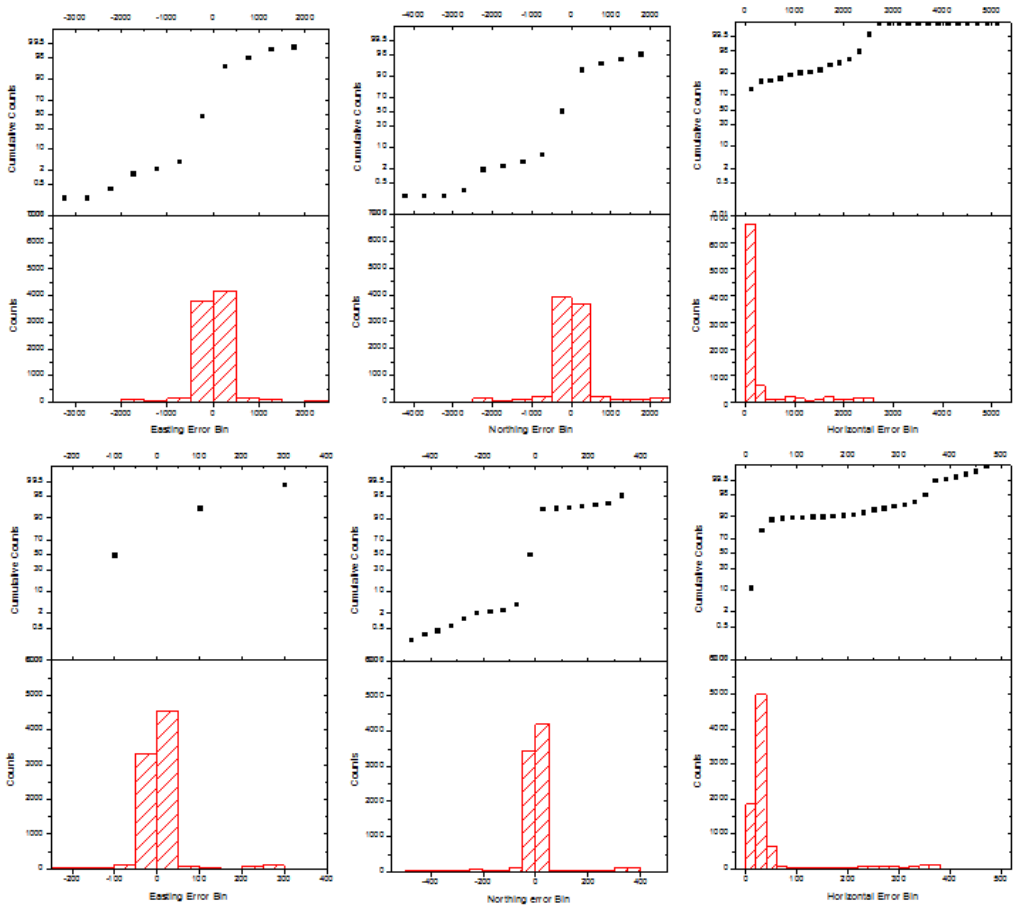

Figure 14 Distribution plot of cellular positioning errors

Table 5 presents the statistical value of the easting, northing and horizontal positioning error. Due to the large sample size, it is assumed that the distribution can be adequately described by the normal distribution; the 95% confidence interval of the measurement error is computed as ±1.96 times the standard deviation. The mean value for easting error and northing error are between 5 m to 6 m, but for horizontal error is between 50 m to 60 m. The standard deviations for both directional and horizontal error are quite large. In general, the relative positioning error of using cellular positioning technology is five times greater than using smartphone GPS positioning technology.

Table 5 Descriptive statistics of cellular positioning error

Mean	Std Dev	Lower Quartile	median	Upper Quartile	Lower 95% CL	Upper 95% CL
All position points						
291.5	622.92	25.85	32.51	63.29	278.39	304.63
Filtered horizontal error						
56.19	82.78	24.67	30.56	36.76	54.29	58.08
Easting error						
5.75	48.35	-11.05	0.589	13.16	4.64	6.85
Northing error						
5.06	87.25	-27.80	-0.67	23.28	6.03	7.06

The vehicle trajectory was constructed using ArcGIS software and projected to Google Earth. The vehicle trajectories shown in Figure 15 consists data points with different colors. Each data point presents a location estimates using cellular positioning. The points were collected in 1 second intervals. Each color represents one distinct cell-ID, and a change of color indicates one handover of the cellphone signal.

Figure 15 Handover points on Whitemud Drive

The figure shows that color changes were observed at several locations along the Whitemud Drive. Comparing the trajectories from different trials, although points of color change from two trials occurs at the same segment on freeway, but they are at different locations ranges from several to tens of meters from each other. As shown in Figure 16, for the same segment, the cell-IDs change from blue to green indicating the phone received signal from two different cell towers.

Figure 16 Example of handover locations

During this experiment, the cell-IDs changed eight times in the first two trails and six times in the last trial, indicating eight and six handover points in the field along the test segment, and the handover points vary among the trials. Each of the approximate handover points is estimated by taking the average of the three locations recorded by the smartphone; their distances to the estimated handover point are considered as errors of the handover-based cellular positioning. An average error of 79.36 m with a standard deviation of 41.07 m was obtained on this segment. The cellular positioning error was found to be within the range of 25-136 m.

The Receiver Signal Strength Indicator (RSSI) for the smartphone is also collected during the test run. RSSI is a radio frequency term, and it is a measure of the power level that a radio frequency device. This figure represents the signal strength to the cellular tower. The plot of RSSI with the data points collected in three trials is presented in Figure 17 below.

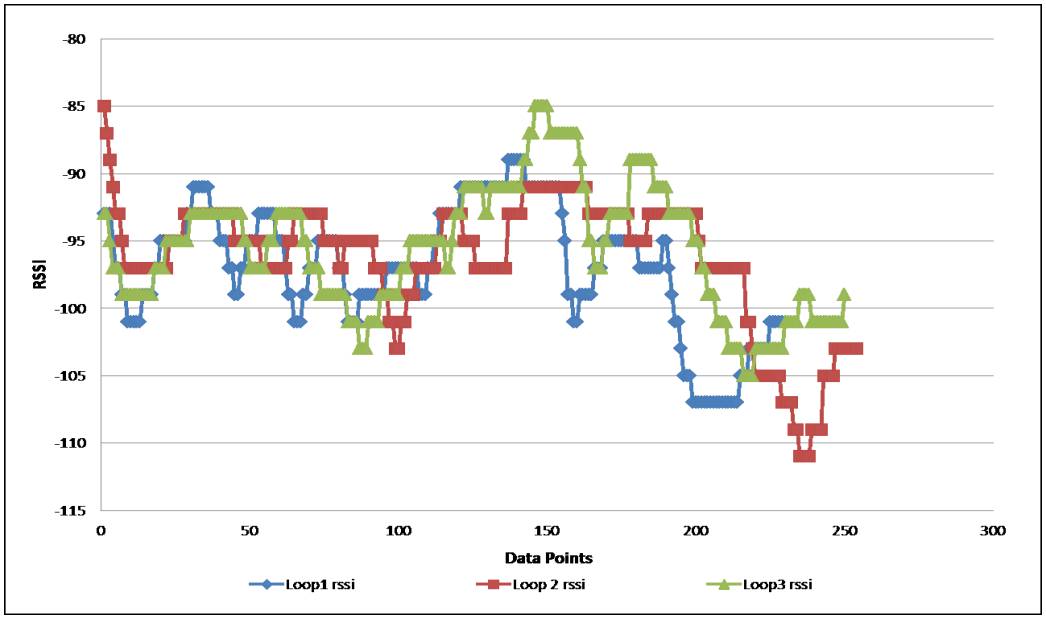

Figure 17 Plot of RSSI along Whitemud Drive

As shown by three colors, the RSSI value varies from -110 dBM to -85 dBM over time at any location, and the signal reception is poor. However, the RSSI trends obtained in all three trials are similar which indicates the validity of the smartphone application. The repeatable trend also can be used with confidence to locate the distance to the cell tower.

Figure 18 below is a close up look at the trajectory recorded using cellular positioning. During the experiment, the vehicle was driving in a straight line along one traffic lane most of the time, and the trajectories obtained using Smartphone GPS are mostly smooth and reflect the vehicle path. However, in the observed trajectory by cellular positioning, some zig-zag patterns are observed at many locations, and in many cases some consecutive points are placed off the road.

Figure 18 Example of cellular positioning trajectory

In summary, the tested cell phone application can record the cell-ID along the test segment; however, the positioning accuracy using cellular positioning technique is much lower than using GPS-enabled smartphones. It is possible to identify the cell coverage using the tested application, although difficulties might arise in certain conditions, such as 1) in the urban area, the cell-ID changes abruptly due to the smaller and frequently overlapped cell coverage; 2) some locations experience poor cellphone signal reception; and 3) at some times and places, the cell-ID trajectories are not identical.

3.3.3 Result for Scenario 3 : GPS-Enabled Smartphone and Geofence

This section analyzes the data collected using Geofences and provides an assessment of Geofence data quality on freeway and arterial. A preliminary test for the Geofence was conducted on July 21st, 2013 along the section of Whitemud Drive from Fox Drive to Anthony Henday. A trajectory is shown in Figure 19 below.

Figure 19 Preliminary Geofence Test Route

During the test, the smart phone receives notification when the vehicle enters the Geofence, the timestamp that the notification was received was recorded by video camera. As shown in Figure 20, vehicle location is then overlaid at that timestamp with the .kml file in Google Earth, and it is observed that the notification message always showed up at the first location point obtained in the Geofence, and most of the time that is within one second entering the Geofence.

Figure 20 Location information for first point entering Geofence

Comparing the data points from the Drivewyze application at twelve Geofence locations and the Juno output, an average error of 3.46 m with a standard deviation of 2.27 m was obtained. Comparing the timestamp of Drivewyze data to the timestamp recorded in the video, a 100% matching rate is obtained and all Drivewyze notification are observed. The positioning error for westbound Geofences are similar to that along eastbound of the test route, and the accuracy level is comparable to positioning using GPS-enabled smartphone alone.

With more data points, it is anticipated that, using this technique, we can accurately find the timestamp of passing any point with known coordinates or vice versa.

A more comprehensive experiment was conducted later to collect more Geofence data. Six different GPS-enabled smartphones were used in this experiment, once they entered the Geofence areas, Geofences were triggered, and all the location data collected within the Geofence were collected and sent to the server.

The location data collected within the Geofences were compared to the location data collected with GPS handset. The relative positioning error for the data collected within Geofences are plotted with timestamp; the box plot, histogram plot and probability plot are shown in Figure 21, and mean position errors for different smartphones are listed in Table 6. The location error for the data collected by IOS smartphones has wider range than others, and that collected using Android phones have smaller error. Among the Android phones, Samsung GS3 and Nexus4 have the least position error.

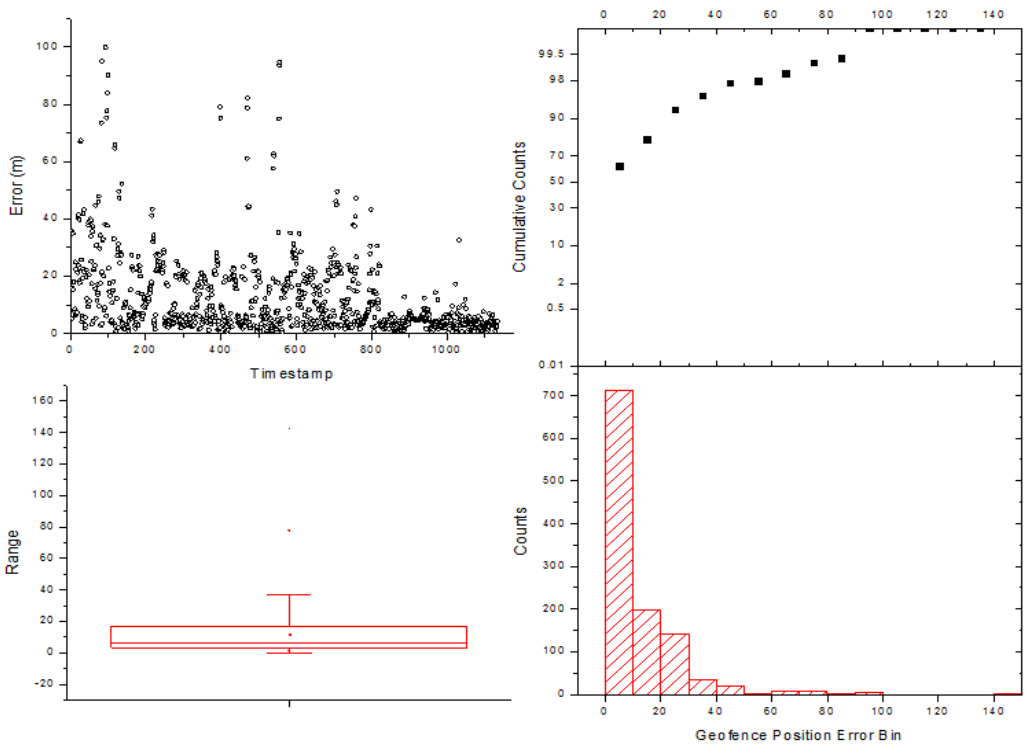

Figure 21 Plot of relative positioning error in Geofences

Table 6 Position error within Geofences for different smartphones

Platform	Android				IOS	
Phone	Samsung GS3	HTC	Nexus4	Samsung Ace	IPhone4S	IPhone 4
Error (m)	4.26	11.94	3.38	4.25	12.32	20.88

3.3.4 Network Delay

Geofence server provides two sets of time information, one indicates the timestamp of when the detection event was triggered, and another is the time where the location information sent by smartphones was received by the server. The difference between the two sets of time is considered the network delay. Plot

of delay data and box plot is shown in Figure 22 below. Histogram plot and cumulative frequency plot are also presented.

The delay plotted with time indicated that most of the network delay is within 20 s. The box plot shows lower and upper quartile of delay is between 5 s to 7.5 s. For all the location points collected within the Geofences, the mean network delay time is 6.64 s, lower and upper 95% confidence intervals are 6.17 s and 7.12 s respectively. From the histogram, 90% of the network delay is less than 10 s, 95% of the network delay is less than 40 s.

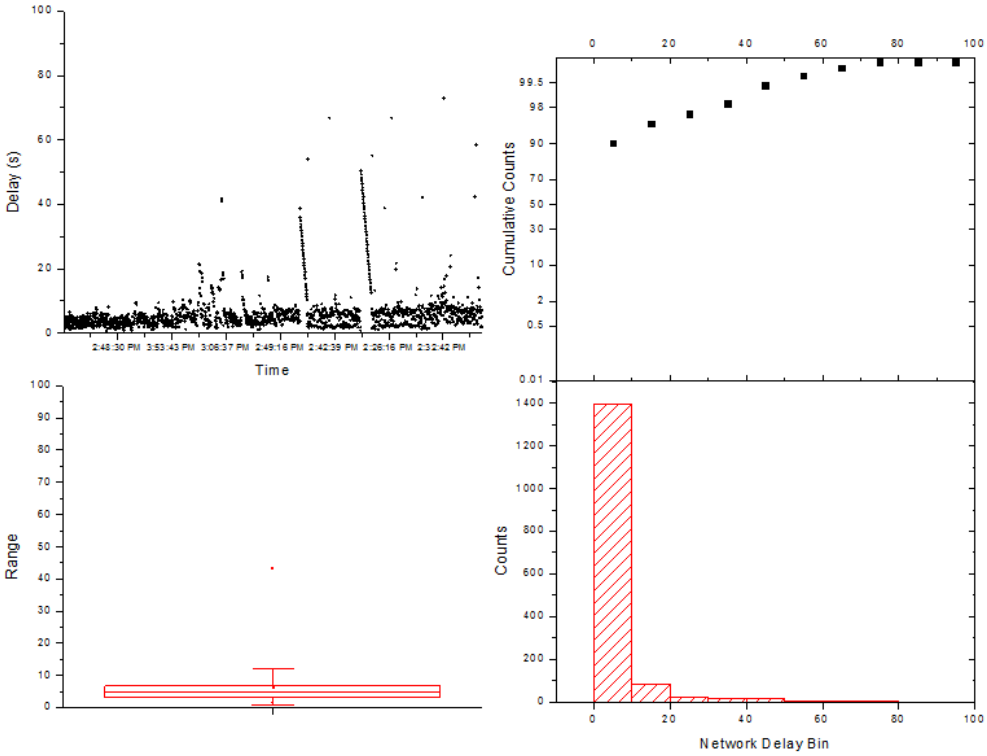

Figure 22 Plot of network delay for all smartphones

The network delay among different smartphones is also compared in Figure 23. The first four plots correspond to Android smartphones, and the last two plots correspond to IPhones with iOS operation system. The delay for

Android smartphones tends to have more outliers than the delay for iOS smartphones.

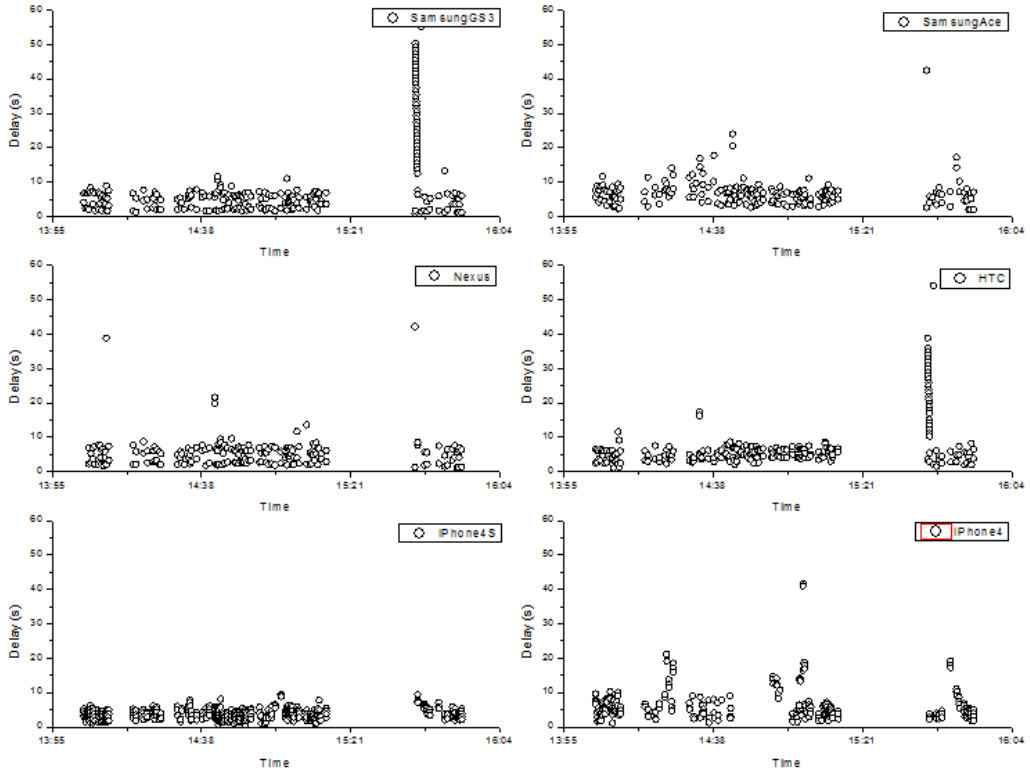

Figure 23 Plot of delay with time for different smartphones

The plot shows at around 3:40 PM, the delay time for Samsung Galaxy S3 and HTC smartphone experienced a steep jump and gradually decreased to more reasonable value. At that timestamp, the vehicle was travelling southbound at the north of intersection of 75 Street and 90 Avenue. These two smartphones first falsely triggered the Geofence on the northbound direction north of the intersection, and then as the vehicle enters the southbound Geofence, the Geofence was correctly triggered by all the smartphones. This may explain the sudden increase of the delay for two of the smartphones.

Some descriptive statistics for network delay are calculated for different phones and presented in Table 7 and Figure 24. From the mean network delay, IPhone4S has the least delay, and SamsungGS3 has the greatest mean delay. From the histograms, the range for iOS smartphones' network delay has smaller range than that of Android smartphones.

Table 7 Network delay for different smartphones

Platform	Android				iOS	
Phone	Samsung GS3	Samsung Ace	Nexus 4	HTC	IPhone 4S	IPhone 4
Mean (s)	9.50	7.43	5.75	7.53	3.65	7.80
St.Dev	12.1	7.20	6.48	7.60	1.55	15.2
Lower95%	7.95	6.42	4.81	6.53	3.50	6.05
Upper 95%	11.05	8.44	6.70	8.51	3.80	9.55

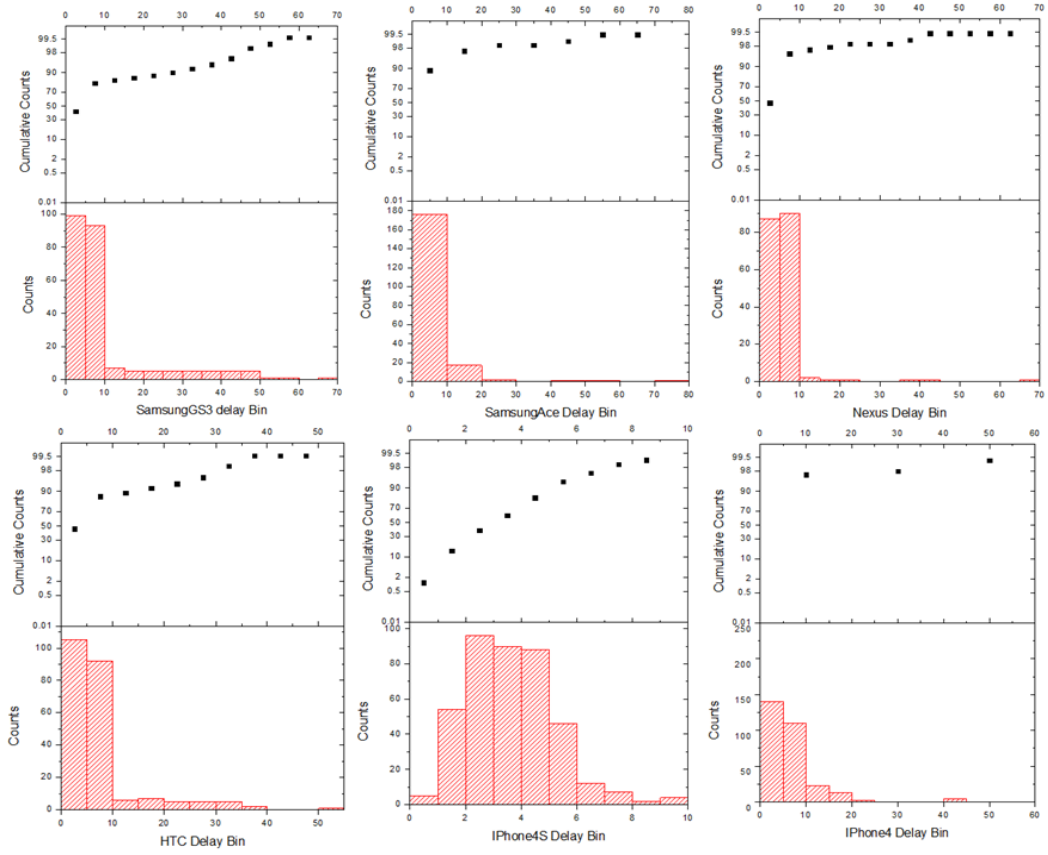

Figure 24 Histogram plot of network delay for different smartphones

3.3.5 Detection Rate

There were 43 Geofences set up on Whitemud Drive, 19 on 170 Street and 34 on 75 Street. As the vehicle drive crosses the Geofence area, the smartphones will receive notification message to indicate detection of a Geofence. However, not all the Geofences were detected by all the smartphones, and some smartphones detected the wrong Geofences. The ratio between the number of Geofences correctly detected by the smartphone to the number of Geofence deployed was referred as detection rate, and the number of times a smartphone falsely indicating detection is referred as false detection. The detection rate is shown in Table 8 blow.

Table 8 Geofence detection rate of different smartphones

Platform	Android				iOS	
Phone	Samsung GS3	HTC	Nexus 4	Samsung Ace	IPhone4S	IPhone4
Total rate	100%	100%	93.8%	100%	100%	76.0%
Whitemud	100%	100%	88.4%	100%	100%	53.5%
170 Street	100%	100%	100%	100%	100%	100%
75 Street	100%	100%	100%	100%	100%	91.2%
False Detection	3	3	2	3	0	0

The result in Table 8 suggests that Android smartphones have higher detection rate than iOS smartphones. Among Android smartphones Nexus4 has the lowest detection rate, and among iOS smartphones IPhone 4 detects the least Geofences. All of the Android smartphones falsely detected the wrong Geofences when waiting for signal lights at an intersection, but none of the iOS smartphones did. This may indicate that iOS smartphones are less sensitive to Geofence setup. Another possible explanation is that when vehicle is waiting at the intersection at

speed of 0, GPS receivers in Android smartphones tends to have location points jump around in the true location in a bigger range than that of iOS GPS receivers, thus triggering the Geofences on the other direction of travel.

3.4 Regression Analysis

In order to have a better understanding on the characteristics of the relative positioning error, this research look at various contributing factors, and investigate their relationship to the magnitude of the positioning errors. In the field for the geometrics, position accuracy is a function not only of the GPS receiver and antenna, but also a function of the geometry and status of the satellites, the surroundings of the antenna, atmospheric and ionosphere conditions. However, when incorporating the GPS positioning techniques to transportation application, most of these factors become less relevant. Therefore, some of these factors are not considered and the scope is limited to traffic and roadway related factors in this research. These factors can be categorized into four groups:

- roadway characteristics
- condition of sight to the satellite
- transportation modes
- other independent variables including vehicle speed, horizontal dilution of precision, and mobile network availability

Some of these factors are considered as independent or explanatory variables that may have an impact on the dependent variable- relative positioning error. Such

independent variables will be tested and introduced into a multiple regression analysis to model their effect on relative positioning error.

3.4.1 Explanatory variables

The following variables are first considered as possible independent variables to be included in to the regression model. Some of these variables take the numeric form, and some of them will be transformed into indicative variables by recoding to binary dummy variables.

HDOP

The horizontal dilution of precision indicates the geometry of satellites; this numeric number allows us to more precisely estimate the accuracy of GPS horizontal position fixes by adjusting the error estimates according to the geometry. In theory, if satellite geometry were the only component of the horizontal error of position, the RMS error would be directly proportional to HDOP. In this regression model, HDOP is tested as one of the numerical independent variables that may impact the error estimation.

Type of facility

The experiments in this research was conducted on various of roadways in City of Edmonton, including segments on freeway, highway, arterial and ramps that connects two type of facilities. For the WMD freeway and QEII highway there is no signalized and un-signalized controls, and all segments are multi-lane. On the urban arterials, the road is narrower with less number of lanes, and signal controlled intersections are spaced unevenly along the corridor. For most of the arterial segments, the road right of way is narrower and adjacent infrastructures

such as buildings and trees are closer to the roadway. The ramps are the connectors between any two of the other three facilities and their characteristics are between the characteristics of the two facilities that it is connected to. Four variables that will be included in the regression model are: freeway, highway, arterial and ramp. Each of them is binary dummy variable, an example of the arterial variable is in the following form:

$$x = \begin{cases} 1 \text{ if the vehicle is on an arterial link at this timestamp} \\ 0 \text{ if the vehicle is not on an arterial link at this timestamp} \end{cases}$$

Speed

The vehicle travel speed during the experiments varies among different road segments and facilities. In general, the arterial travel speed should be between 0 to 60km/h, freeway travel speed is between 0 to 80km/h, and highway travel speed is between 0 to 100km/h. From the smartphone GPS data, the estimated speeds at all timestamps range from speed of 0 to speed of above 140 km/h.

Sight to satellite

Direct sight between the GPS receiver and the satellites is required to correctly identify the location of the GPS receiver. Since most of the data points were collected in passenger vehicle and in bus, the sight to satellite is referred as the open sky condition above the roof of the vehicle. In the areas where streets are surrounded by high-rise buildings or where vehicles travel under the tunnel, the sight to the satellite is limited, and data collected under this condition is categorized under dummy variable limited sight. Streets with tall trees or mid- rise buildings on the sides is considered as partially open sky, and data collected under this condition is captured by dummy variable called partial sight. Areas such as

river crossing and city ring road has no building or trees on the sides are considered as full open sky with direct sight to the satellite, this condition is categorized as dummy variable called full sight to satellite.

Mode of transportation

Three modes of transportation are used in this study: passenger car, bus, and walk. The trips made during the experiments are not necessary made by using one mode of transportation. In some cases, mode transfer happens once or twice during the same trip. Dummy variables of car, bus and walk are set up for each of these three modes.

Mobile Network

Many of the GPS-enabled smartphones in nowadays provides the users the option to use mobile network when obtaining location services. If the mobile network option is not turned on, the location information will only be collected using the GPS receiver embedded. When the mobile network option is enabled, the device will also use cellular network and/or wireless communication network to aid the GPS positioning. Combining the GPS positioning with mobile network will help to locate the device faster and with higher accuracy. A binary dummy variable is used to distinguish the data collected with or without the mobile network option enabled.

Stop

During the experiment, vehicle was stopped several times at signalized intersections on urban arterials, or queued due to traffic congestion. During that short period, the smartphone GPS receiver is in stationary status, and the relative

position error may be impacted due to this change. A binary variable is assigned in the model to capture the impact of this factor.

3.4.2 Correlation Analysis

At the first step of the statistical analysis, correlation analysis was performed to study the relationship between the relative positioning error, and some transportation related explanatory variables. Correlation coefficients which are the result of correlation analysis range from -1 to +1. Correlation coefficient with the value of zero represents no relationship between variables while correlation value of -1 means strong negative relationship and correlation coefficient of +1 represents a strong direct relation. The closer is the correlation coefficient to +1, it shows the stronger relation. Correlation coefficients between the aforementioned variables were calculated using SAS software and the results are illustrated in Table 9.

Table 9 Correlation analysis

Variable	Correlation	Pr >|t|
Speed	-0.27946	<.0001
HDOP	0.16153	<.0001
Highway	-0.27256	<.0001
Freeway	-0.16904	<.0001
Arterial	0.39071	<.0001
Ramp	-0.0802	<.0001
Bus	0.25826	<.0001
Car	-0.24398	<.0001

Walk	-0.00838	0.2268
Stop	0.05924	<.0001
Full Sight	-0.29244	<.0001
Partial Sight	0.22997	<.0001
Limited Sight	0.13328	<.0001
Mobile Network	-0.29608	<.0001

According to the results, HDOP, arterial, partial and limited sight to the satellites, bus, stop and positioning error showed positive correlation. This implies that the relative positioning error will likely to increase if these variables with quantitative values increases or these dummy variables have value of 1. Among those the correlation coefficients for arterial and partial sight to the satellites showed higher correlation in comparison to the others. Among the negatively correlated variables speed, highway, car, full sight and mobile network has greater correlation with relative position error than others. There is no extreme correlation between pairs of variables. Variables including ramp, walk, and stop has small coefficients showing almost no correlation.

3.4.3 Regression Analysis

Regression analysis was performed to model the relationship between relative positioning error and aforementioned variables. Multilinear regression models are estimated to investigate the relationship between the aforementioned independent variables and the GPS-enabled smartphone relative position error, and to quantify the impact that these factors may have on the positioning error.

Since the normality test indicates that the natural log of relative position error most likely follows a normal distribution, the error itself must follow a log normal distribution. The probability density function (PDF) of a log-normal distribution is:

$$f_X(x;\mu,\sigma) = \frac{1}{x\sigma\sqrt{2\pi}} e^{-\frac{(\ln x-\mu)^2}{2\sigma^2}}, x > 0$$

The multivariable linear regression model takes the following form:

$$\ln(Error) = \alpha_0 \times X_0 + \alpha_1 \times X_1 + \alpha_2 \times X_2 + \alpha_3 \times X_3 + ... + \alpha_n \times X_n + \varepsilon$$

Where:

$X_1, X_2, \ldots\ldots X_n$ are the explanatory variables, and stand for the model inputs

α_1, α_2 …. α_n are the coefficients for explanatory variables

α_0 captures the combined effect of omitted variables and x_0=0.

ε is the error term that captures the random effect of error

Explanatory variables mentioned in the correlation analysis are all used to model the relative position error. Three common heuristic subset selection method including forward selection, backward selection, and stepwise regression are used. A number of criterions have been used for deciding which variable to add or remove at a given step in the regression process as well as when to quit adding or removing the variables. Adding additional variables will always increase the R square of the fit and including too many variables may increase multicollinearity and results in numerically unstable models. So use of information criterions will help balance maximizing the fit while protect against overfitting. The criteria used in the model selection are Akaike's Information Criterion (AIC), Sawa's Bayesian

Information Criterion (BIC), and Schwarz's Bayesian Information Criterion (SBC). Three model diagnostic statistical techniques including R-square, adjusted R-square, and Mallows C(P) are also used to determine the best linear model [44]. Their formulas are shown below:

Table 10 Model fit summary statistics

Model Option	Formula
R Square	$1\text{-}\frac{SSE}{SST_I}$
Adjusted R Square	$1-\frac{(\mathrm{n}-i)(1-R^2)}{n-p}$
CP	$\frac{SSE}{\sigma^2}+2p-n$
AIC	$n\ln(\frac{SSE}{n})+2p$
BIC	$n\ln(\frac{SSE}{n})+2(p+2)q-2q^2 whereq=\frac{n\sigma^2}{SSE}$
SBC	$n\ln(\frac{SSE}{n})+p\ln(n)$

Linear regression results

The fourteen variables included in the correlation test are all considered in the regression model. To avoid multicollinearity, one variable from each of the first three categories is removed from the model at the beginning. The dropped explanatory variables are ramp, full sight, and walk. The regression results of

using three heuristic methods are very similar, the results from stepwise regression method is presented here.

The best fit criteria plots are shown in Figure 25. The first criteria selects the best model form based on reaching the maximum value, and the following four criteria selects the model based on minimizing the value. The criteria values improve incrementally in each step, and all of the criteria reached their optimum value, and best model is selected with parameter estimates listed in Table 11.

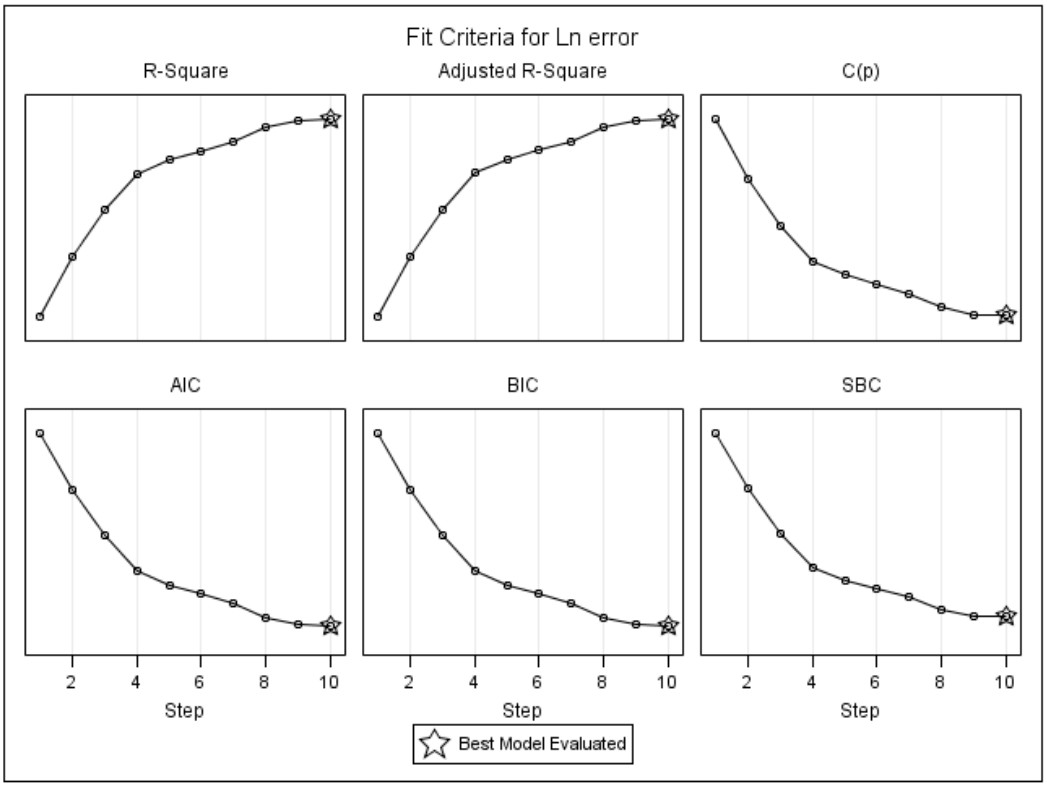

Figure 25 Plot of fit criteria

Table 11 Parameter Estimates for Linear Regression Model

Notation	Variable	Parameter Estimate	t value	Pr >|t|
x_0	Intercept	1.22952	24.35	<.0001
x_1	Speed	0.00517	17.6	<.0001
x_2	HDOP	0.00883	17.21	<.0001
x_3	Car	0.15783	3.54	0.0004
x_4	Bus	0.60282	13.1	<.0001
x_5	Freeway	-0.36439	-12.89	<.0001
x_6	Arterial	0.30568	12.7	<.0001
x_7	Highway	-0.39865	-14.34	<.0001
x_8	Limited Sight	0.33617	13.68	<.0001
x_9	Partial Sight	0.1247	8.04	<.0001
x_{10}	Mobile Network	-0.33358	-22.93	<.0001

The multivariable linear regression model takes the following form:

$$\text{Relative Positioning Error} = \text{Exp} \sum_{i=0}^{i=10} \alpha_i x_i + \varepsilon$$

Where i= 0, 1, 2, …..10

x_i= variables values

α_i= parameter estimate

ε = error term

Eleven parameters are remained in the regression model, and the degree of freedom of this model is 10. R-square value for this model is 0.2216 and the adjusted R-square is 0.2212 indicating the considered variables accounts for 22% of the variation in the captured relative positioning error. Since many of the variables considered in the model are binary indicated measures, a small R-square

value is reasonable. The F value for the model is 592.43 and Pr>F value is less than 0.0001 indicating that the model is significant. In this regression analysis, the confidence interval is set to be 95%, therefore if the significance value of a parameter estimate is less than 0.05 the independent variables are considered significant. All of the eleven parameter estimates listed in Table 11 are less than 0.05 indicating that all explanatory variables remaining in the model are significant at 95% confidence interval. Since most of them are less than 0.0001, the parameter estimates in this model are considered as highly significant. Some of the estimates are positive numbers indicating positive impact on the magnitude of error where some negative estimates indicate negative impact.

The parameter estimates for vehicle speed is positive, which means increasing of vehicle speed will increase the relative position error, and by increasing the speed by one unit while other variables are held constant, the position error will increase 1.005 times (exp0.00517). This estimate is reasonable since as the speed increases, the distance traveled over one timestamp will be greater, and the error for estimated position will therefore increase accordingly.

The parameter estimates for HDOP is positive indicating increasing HDOP will also increase the positioning error. Since a high HDOP value indicates that the geometry of the satellites is poor, increasing HDOP value will result in a lower positioning accuracy, hence higher positioning error.

The parameter estimates for freeway and highway are all negative and for arterial is positive. This illustrates the fact that in comparison to the position error collected at on ramps and off ramps, position error for data collected on arterial

road link is around 35.7% (exp0.305) higher, error for data collected on freeway and highway will be 30% lower.

In comparison to error collected under full sight to satellite condition, the relative positioning error for data collected under limited sight condition will be 40% higher, and that under partial sight condition will be 13% higher.

Compare to the error collected by walking, the position error will increase by 17% if the data are collected in a moving car, and that will increase by 83% if the data is collected by taking a bus.

In comparison to the position error for data collected solely using smartphone GPS, the relative error for data collected with accompany of mobile network is 30% lower.

The parameter estimates suggests that the intercept value is also significant, indicating that there may be some other variables significant to the error estimation but are not captured in this model, therefore, their effects are captured by the constant term. The parameter estimates for all the variables are in concordance with intuitive perception.

3.4.4 Multicollinearity Analysis

In multiple regression models, the most severe problem is the multicollinearity. Multicollinearity is a statistical phenomenon refers to the presence of higher inter-correlated predictor variables in regression models. To avoid this problem, collinearity diagnostics was conducted to measure how much regressors are related to other regressors and how it will affect the stability and variance of the regression estimates. If the above regression model has a multicollinearity

problem, model parameters need to be refined. The criteria set for indicating the existence of multicollinearity problem in this study are: large standard error for parameter estimates, Variance Inflation Factor (VIF) greater than 10, detection – tolerance less than 0.1, as well as condition number test greater than 30. In the above regression model with degree freedom of 10, the result for collinearity diagnostics are listed in Table 12.

Table 12 Collinearity Diagnostics

Parameter	Standard Error	Tolerance	Variance Inflation	Condition Index
Intercept	0.05049	.	0	1.00000
Speed	0.00029374	0.25186	3.97049	1.64639
HDOP	0.00051327	0.96326	1.03814	2.10355
Car	0.04456	0.10696	9.34947	9.79479
Bus	0.04601	0.10971	9.11512	10.73503
Freeway	0.02827	0.3654	2.7367	2.2422
Arterial	0.02408	0.20765	4.81585	2.28457
Highway	0.02779	0.19971	5.00723	2.99331
Limited Sight	0.02457	0.72434	1.38057	4.30357
Partial Sight	0.01552	0.54331	1.84056	5.72607
Mobile Network	0.01455	0.76954	1.29947	26.447

As shown in the table, the standard errors for 11 parameter estimates are all small. All of the tolerance value are greater than 0.1. None of the condition number corresponding to independent variables is greater than 30. Finally the VIF

values for all of the independent variables are less than 10, indicating that there is no perfect multicollinearity observed in the above regression model.

3.4.5 Regression analysis with speed dummy

We have observed that vehicle speed is correlated with relative positioning error of the GPS-enables smartphones, and the parameter estimate is significant. Knowing that the speed has positive impact on the positioning error, it is feasible to investigate further on the extent of such impact by certain speed or speed ranges. To achieve this, we undertook recoding process to convert vehicle speed from one quantitative variable to a set of indicator variables.

Speed was divided into 15 bins where the first speed bin covers speed from 0 to 10 km/h, last speed bin covers speed greater than or equal to 140 km/h, and each of all other speed bins covers a range of 10 km/h. Each of these speed bins are treated as binary dummy variables, and were used to capture the stepwise effect of speed on GPS positioning relative error. One speed dummy was removed before using the regression to prevent multi-collinearity. The speed dummy variables are defined as follows:

- Variableδ_1: Speed 0-10km/h $\begin{cases} D = 1 \text{ if speed } \leq \frac{10\text{km}}{\text{h}} \text{is true} \\ D = 0 \text{ if speed } \leq \frac{10\text{km}}{\text{h}} \text{is not ture} \end{cases}$
- Variableδ_2: Speed 10-20 km/h $\begin{cases} \text{D} = 1 \text{ if } \frac{10\text{km}}{\text{h}} < \text{speed } \leq \frac{20\text{km}}{\text{h}} \text{is true} \\ \text{D} = 0 \text{ if } \frac{10\text{km}}{\text{h}} < \text{speed } \leq \frac{20\text{km}}{\text{h}} \text{is not ture} \end{cases}$

  …….
  …….
- Variableδ_{15}:Speed >140 km/h $\begin{cases} D = 1 \text{ if speed} > \frac{140\text{km}}{\text{h}} \text{is true} \\ D = 0 \text{ if speed} > \frac{140\text{km}}{\text{h}} \text{is not ture} \end{cases}$

Other independent variables from the previous regression model remains in this new regression. Using the stepwise regression method, a linear regression model is obtained and the list of parameter estimates is shown in Table 13. Similar to the previous mode, to avoid multicollinearity, one dummy variable in each category is dropped from the model, and the dropped explanatory variable in the speed category is δ_1.

Table 13 Parameter Estimates for Linear Regression Model

Notation	Variable	Parameter Estimate	t value	Pr >|t|
x_0	Intercept	1.26289	41.13	<.0001
x_1	HDOP	0.00825	16.22	<.0001
x_2	Stop	0.12188	3.93	0.0001
x_3	Bus	0.48434	25.13	<.0001
x_4	Freeway	-0.2219	-7.55	<.0001
x_5	Arterial	0.22478	9.33	<.0001
x_6	Highway	-0.29328	-8.93	<.0001
x_7	Limited Sight	0.34476	14.18	<.0001
x_8	Partial Sight	0.12348	8.07	<.0001
x_9	Mobile Network	-0.32733	-22.73	<.0001
δ_2	Speed 10-20	0.21383	7.1	<.0001
δ_3	Speed 20-30	0.30865	10.53	<.0001
δ_4	Speed 30-40	0.50764	18.57	<.0001
δ_5	Speed 40-50	0.55538	20.97	<.0001
δ_6	Speed 50-60	0.61155	22.64	<.0001
δ_7	Speed 60-70	0.50853	17.4	<.0001
δ_8	Speed 70-80	0.38883	12.34	<.0001
δ_9	Speed 80-90	0.3428	10.46	<.0001
δ_{10}	Speed 90-100	0.35891	9.83	<.0001

δ_{11}	Speed 100-110	0.69608	17.64	<.0001
δ_{12}	Speed 110-120	0.60107	15.11	<.0001
δ_{13}	Speed 120-130	0.45398	8.74	<.0001

The multivariable linear regression model takes the form of :

$$\text{Error} = \text{Exp}\left(\sum_{i=0}^{i=9} \alpha_i x_i + \sum_{j=2}^{j=13} \beta_j \delta_j \right) + \varepsilon$$

Where i= 0, 1, 2, …..9

x_i= first 10 variables listed in Table 13

α_i= parameter estimate for corresponding first 10 variables

δ_j= speed dummy variables

β_j= parameter estimates for speed dummy variables

ε = error term

There are 22 parameters estimated in this model, and the degree of freedom of this linear model is 21. R- square value for this model is 0.2432 and adjusted R-square is 0.2425 indicating the considered variables accounts for 24% of the variation in relative error. Since most of the variables considered in the model are binary dummy variables, a small R-square value is reasonable. The F value for the model is 318.37 and Pr>F value is less than 0.0001. In this study, the confidence interval is set to be 95%, therefore, a significance values less than 0.05 indicates that the independent variables is significant and there is a considerable relationship between the dependent and independent variable. The probability value for the parameter estimation are all less than 0.05, indicating all explanatory variables remaining in the model are significant at 0.05 significance level. Most of

them are less than 0.0001 indicating that all the variables in this model are highly significant.

All of the parameter estimates for speed between 10 km/h to 130 km/h are positive indicating position estimate data collected at these speeds have higher value of error in comparison to those collected at speed less than 10 km/h. As speed increases, the position error is likely to increase. For different range of speed, their impacts to the positioning error will be different. For example, holding other variables constant, if all other factors are identical, when speed is between 20 km/h and 30 km/h, the positioning error will be 1.238 (exp0.213) times higher than if the speed is between 10 km/h to 20 km/h. When speed is between 100 km/h and 110 km/h, the positioning error will be 1.401times higher than if the speed is between 90 km/h and 100 km/h. If the speed is in the range of 20 km/h to 30 km/h, increase speed by 1 km/h will result in 23.8% increase of relative position error. When speed is between 100 km/h and 110 km/h, for every speed increment of 1km/h, the positioning error will be doubled (exp0.695). The effect of different vehicle speed on relative position error is plotted in Figure 26.

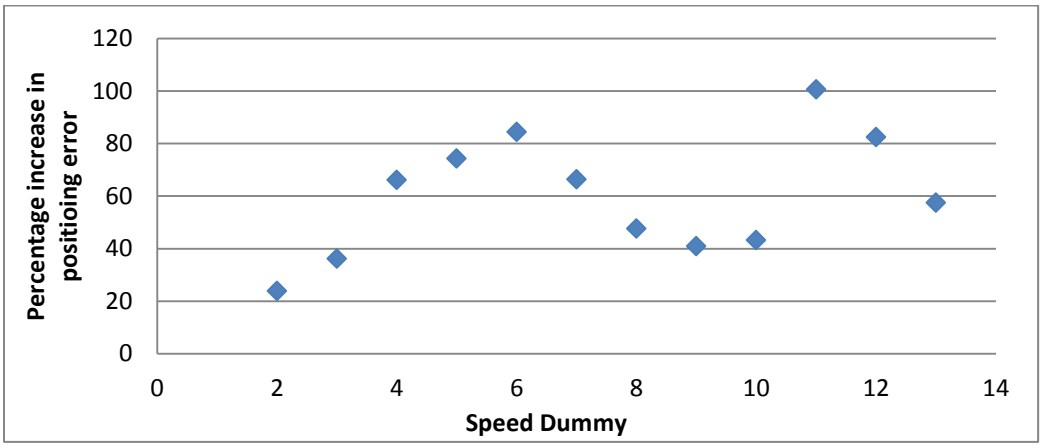

Figure 26 Effect of different speed on relative position error

For speed below 60 km/h, as speed range increases, the impact on relative position error will increase almost linearly. For speed range between 60 km/h and 90 km/h, increasing speed range will result a decrease of the impact on position error. For speed range of between 110 km/h and 140 km/h, increase speed range will lead to decrease of the impact on error again.

In previous regression, independent variable of collecting data by car is significant, and variable of stop is not significant and is removed in the regression progress; however, in this regression the variable of car is not significant and variable stop is added into the model instead. The parameter estimate of 0.12 indicates that in comparison to position error collected when vehicle is moving, the error will be less if the vehicle is in stationary condition. The sign of all other parameter estimates are identical to the estimates in the previous regression. The magnitude of all other parameter estimates are also similar except the estimates for freeway, arterial and highway are smaller indicating their effect on relative position error are reduced. A collinearity diagnostics was also performed for the above regression model with degree freedom of 21, the result for collinearity diagnostics are listed in Table 14.

Table 14 Collinearity Diagnostics

Variable	Standard Error	Tolerance	Variance Inflation	Condition Index
Intercept	0.03071	-	0	1
HDOP	0.00050835	0.95519	1.04691	2.19522
Stop	0.03105	0.64459	1.55138	9.84116
Bus	0.01928	0.60799	1.64475	5.95525

Freeway	0.02939	0.32876	3.04177	2.24972
Arterial	0.02408	0.20194	4.95204	3.20458
Highway	0.03286	0.13901	7.19387	3.38242
Limited Sight	0.02432	0.71918	1.39046	3.80293
Partial Sight	0.01531	0.54289	1.84201	5.49324
Mobile Network	0.0144	0.76359	1.3096	14.23092
Speed 10-20	0.0301	0.6418	1.55812	1.39389
Speed 20-30	0.02932	0.62327	1.60444	1.61663
Speed 30-40	0.02734	0.56674	1.76449	1.93092
Speed 40-50	0.02649	0.5047	1.98137	1.98295
Speed 50-60	0.02701	0.45129	2.21589	2.09233
Speed 60-70	0.02922	0.50424	1.98319	2.10376
Speed 70-80	0.0315	0.37744	2.64939	2.1048
Speed 80-90	0.03276	0.39519	2.53041	2.10526
Speed 90-100	0.03652	0.37479	2.66814	2.10528
Speed 100-110	0.03945	0.23272	4.29697	2.10528
Speed 110-120	0.03978	0.20777	4.81292	2.10528
Speed 120-130	0.05197	0.53238	1.87836	2.10528

Similar to the result of the previous collinearity diagnostics, the standard errors for all variables are small. The tolerance value are all greater than 0.1. The variance inflation values are all less than 10, and no condition index is greater than 30. Hence, no sign of multicollinearity is observed for this regression model.

CHAPTER 4. SMARTPHONE GPS POSITIONING IN TRAFFIC STATE ESTIMATION

This chapter introduces the experimental design, and calculation algorithm of using GPS-enabled smartphones and Geofence for traffic state estimation. The experimental results are presented, and performance of different smartphones is also discussed.

4.1 Introduction

This chapter presents a methodology for collecting and analyzing traffic state information using smartphone GPS and Geofence concepts.

The goals of this experiment are to:

- Assess the feasibility of capturing traffic state variables using GPS-enabled smartphone and Geofence concept on freeway and arterials in City of Edmonton.
- Evaluate the accuracy of estimated speed and travel time measurements and compare the estimates from different smartphones to ground truth values from video camera and loop detectors.

To reach the goals for this experiment, the analysis includes obtaining the location of a vehicle at a certain timestamp, the time of traversal with a known location on the vehicle trajectory, as well as average speed and link travel time on the roadway segments.

4.2 Experimental Design

This part of the experiment is conducted along Whitemud Drive and 170 Street. The deployment locations of Geofences are already described in Chapter 3. We used existing roadside infrastructures such as overhead signposts, overpasses, railway crossings, and intersection downstream traffic lights etc. as reference lines within the Geofence areas. For freeway segments, the spacing for reference lines varies within a larger range compared to those on arterial segments. This is due to the fact that the roadside infrastructures on freeways are not distributed evenly, and roadside infrastructures at intersections are more evenly spaced on arterial segments. When calculating the timestamp difference of a vehicle crossing a reference line, or the position error of the smartphone GPS at that timestamp, we used the front passenger seat as the point of reference for the trajectory of that vehicle. The Geofences were set up such that at least one GPS fix is obtained before and after the reference lines, so that the traffic information at that point can be estimated. An example of Geofence set up and notation of obtained location data is shown in Figure 27.

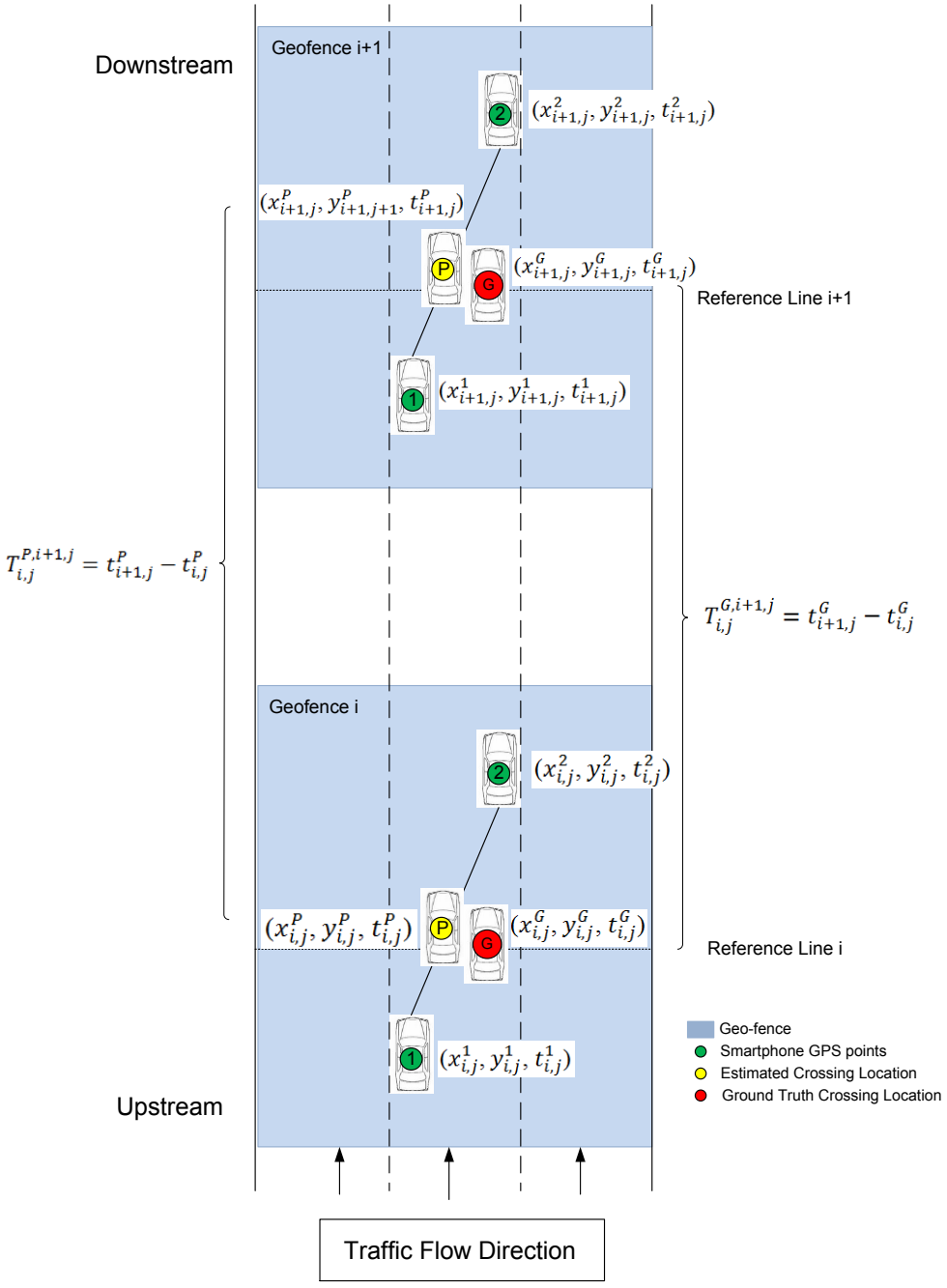

Figure 27 Example of data collection by Geofence

The figure shows the configuration of a three lane road segment. The vehicle is travelling in the middle lane and enters two Geofences i and i+1 shaded in blue. The location information collected within Geofence is indicated beside the vehicles. The distance between the two consecutive reference lines is denoted

as road link distance. The travel time between the timestamp of crossing two reference lines is the link travel time. Figure 28 presents the details of the vehicle locations in an X-Y co-ordinate system, where x axis is the easting value, and y axis is the northing value. Vehicle with point 1 and 2 in green represents the GPS location points before and after the reference line respectively. Vehicle with point G in red represents the ground truth location of the vehicle when crossing the reference line. Point 1 and 2 are used to construct a straight line which is part of the vehicle trajectory. The equation of this trajectory line can be obtained by using a system of two linear equations. In most cases the ground truth point G is not on the line of trajectory, and point G can be projected onto point P shown in yellow on the trajectory line by constructing a perpendicular line to the line of trajectory. Point G and P forms line 2, and coordinates for point P can be obtained using the two linear equations of the lines.

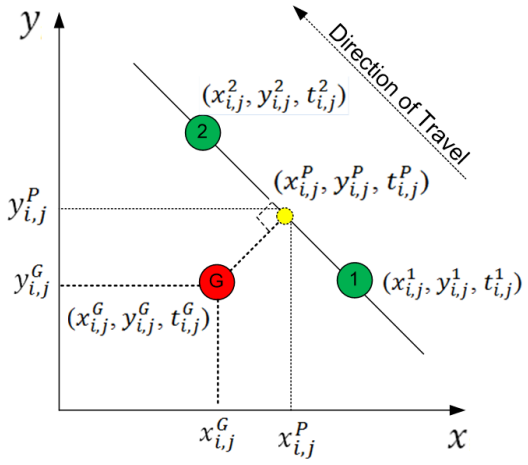

Figure 28 Timestamp of passing reference point

Time stamp error at known location

When point 1 and 2 are identified, point P can be projected to a position between points 1, 2 or outside of the connection between 1 and 2. In either case, the travel time among any of point 1, 2, and P can be obtained in the same way. As a vehicle crosses a reference line, the crossing timestamp is recorded by video, and is used as the ground truth timestamp $t_{i,j}^{G}$. Smartphone with GPS receiver will record the nearest location point right before and after crossing the reference line and the timestamp at crossing $t_{i,j}^{P}$ can be calculated. Comparing the calculated timestamp with the ground truth timestamp, the timestamp difference can be obtained. The highest frequency of obtaining GPS fixes is set at 1 second, and it is assumed that the traffic condition within one second does not change and the vehicle moves at a constant speed in this second.

The distance between point 1 and 2 is

$$D_{12} = \sqrt{(x_{i,j}^{2} - x_{i,j}^{1})^{2} + (y_{i,j}^{2} - y_{i,j}^{1})^{2}}$$

The ratio of distance between point 2 and P, to distance between point 1 and 2 is

$$\frac{D_{2P}}{D_{12}} = \frac{(t_{i,j}^{2} - t_{i,j}^{p}) \times (v_{i,j}^{2} - v_{i,j}^{p})}{(t_{i,j}^{2} - t_{i,j}^{1}) \times (v_{i,j}^{2} - v_{i,j}^{1})}$$

Where D is the distance between two points, and v is the speed of the vehicle.

From above equations, timestamp of crossing the reference line for Geofence i along corridor j can be obtained.

Horizontal error at known timestamp

At a given timestamp of crossing a reference line, the estimated location of the vehicle can be compared to ground truth location. A video camera was used to record the ground truth vehicle trajectory and GPS-enabled smartphones records location points, and the vehicle trajectory can be imported to Google Earth, and the location of vehicle crossing the reference line can be estimated. At a reference point, the ground truth point is assumed to be the middle point of the lane, and the estimated vehicle location from vehicle trajectory can be compared to the ground truth location. The differences between the X coordinates and Y coordinates of the ground truth point and the estimated point are denoted by ΔX and ΔY. X is the easting coordinate and Y is the northing coordinate. The distance between the ground truth point and the estimated point can be obtained by

$$D_{GF} = \sqrt{(x_{i,j}^{G} - x_{i,j}^{P})^2 + (y_{i,j}^{G} - y_{i,j}^{P})^2}$$

Travel Time Estimation

The link travel time between two consecutive Geofences is the duration of the vehicle traverses that link. It is obtained by calculating the difference in time of the vehicle passing the start and end points of a link. The link defined in this experiment starts from the start point of the first Geofence and ends at the start point of the next Geofence in the downstream. The link travel time is denoted by the following equation:

$$T_{\mathrm{i,j}\rightarrow\mathrm{i+1,j}} = t_{\mathrm{i+1,j}} - t_{\mathrm{i,j}}$$

The timestamps from GPS enabled smartphone were used when calculating the estimated link travel time, and the ground truth timestamps were used to calculate the ground truth travel time. The difference between the two link travel times is denoted as

$$\Delta T_{\mathrm{i,j,}\rightarrow \mathrm{i+1,j}} = T^{P}_{\mathrm{i,j,}\rightarrow \mathrm{i+1,j}} - T^{G}_{\mathrm{i,j,}\rightarrow \mathrm{i+1,j}}$$

The total travel time along the trajectory path is the cumulative of the link travel times.

$$T_{pathj} = \sum_{i=1}^{n} T_{i,j\rightarrow i+1,j}$$

The difference between the total travel times can be obtained as

$$\Delta T_{pathj} = \sum_{i=1}^{n} T^{P}_{i,j\rightarrow i+1,j} - \sum_{i=1}^{n} T^{G}_{i,j\rightarrow i+1,j}$$

Travel Speed Estimation

The average travel speed a vehicle uses to traverse the link is calculated by dividing the distance of the link by the link travel time. The estimated link travel time and ground truth travel time were used to obtain the estimated link travel speed and ground truth link travel speed respectively.

$$V_{i,j\rightarrow i+1,j} = \frac{D_{i,j\rightarrow i+1,j}}{T_{i,j\rightarrow i+1,j}}$$

The average travel speed along the corridor j is calculated as the average of the summation of the link travel speeds

$$V_{avg} = \frac{1}{n}\sum_{i=1}^{n}(D_{i,j\rightarrow i+1,j} / T_{i,j\rightarrow i+1,j})$$

The difference between the estimated and ground truth average travel speeds is denoted by

$$\Delta V_{avg} = \frac{1}{n}\sum_{i=1}^{n}(D^{P}_{i,j\to i+1,j}/T^{P}_{i,j\to i+1,j}) - \frac{1}{n}\sum_{i=1}^{n}(D^{G}_{i,j\to i+1,j}/T^{G}_{i,j\to i+1,j})$$

Compare to loop detector data

Point-based speed data are usually extrapolated over roadway segments to estimate the speed for the entire roadway, and to estimate travel times for longer corridors. The simplest approach used widely around the world is to assume the speed for road links are constant [45, 46, 47]. A simple modification to this approach is to assume the speed is piecewise constant between measurement points [48, 49]. In this experiment, a linear speed interpolation method proposed by Van Lint and van der Zijpp is used to estimate the point speed measures at Geofence locations using loop detector point speeds.

The analytical equation for this linear speed interpolation is

$$V_{\mathrm{m}\to m+1}(x) = v_m + \frac{x_{geo} - x_m}{x_{m+1} - x_m} \times (v_{m+1} - v_m)$$

Where

x is the distance measure along the corridor

m is the m th loop detector on the corridor

v is the point speed detected by loop detectors m and m+1

V is the estimated point speed at any point between loop detector m and m+1

The point speeds at the Geofence locations are estimated by smartphone collected location data and by using interpolation of the loop detector data. Two sets of speed will be compared.

4.3 Experimental Results

The field test route in this part of the experiment includes sections of Whitemud Drive freeway, and urban arterial 170 Street.

4.3.1 Whitemud Drive

The section of Whitemud Drive traversed is between 170 Street and 75 Street. There are 43 Geofences set up on this 14.8 km stretch of freeway. The location of the Geofences is shown in Figure 29. The Geofence spacing varies from 168 m to 1200 m on this stretch of freeway.

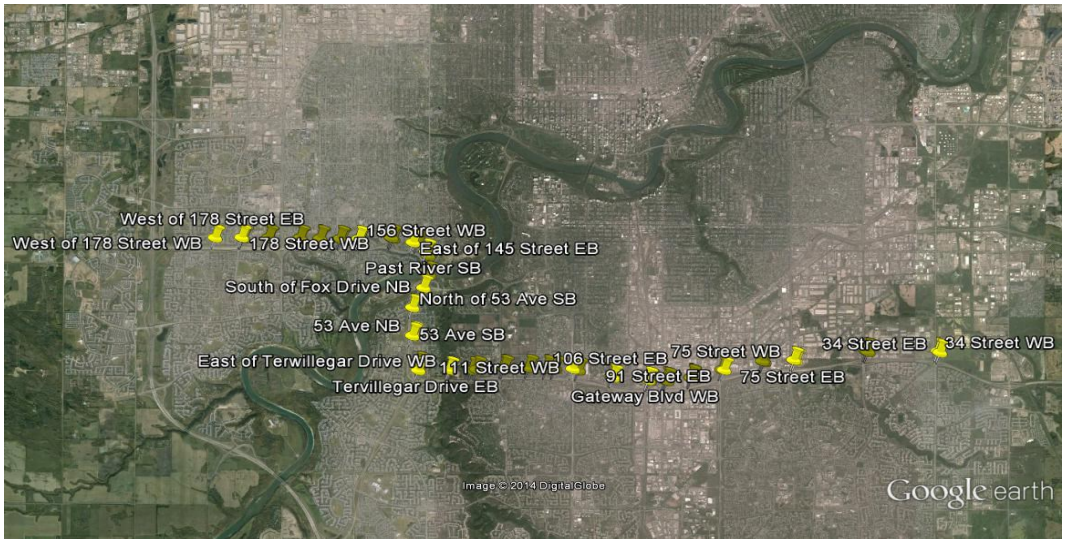

Figure 29 Geofence locations on Whitemud Drive

The location where the vehicle traverses the Geofence is recorded by the smartphone GPS, the easting and northing coordinates were compared to the ground truth crossing locations. The easting and northing error for all the

smartphones and the distance between the estimated and true locations are plotted in Figure 30.

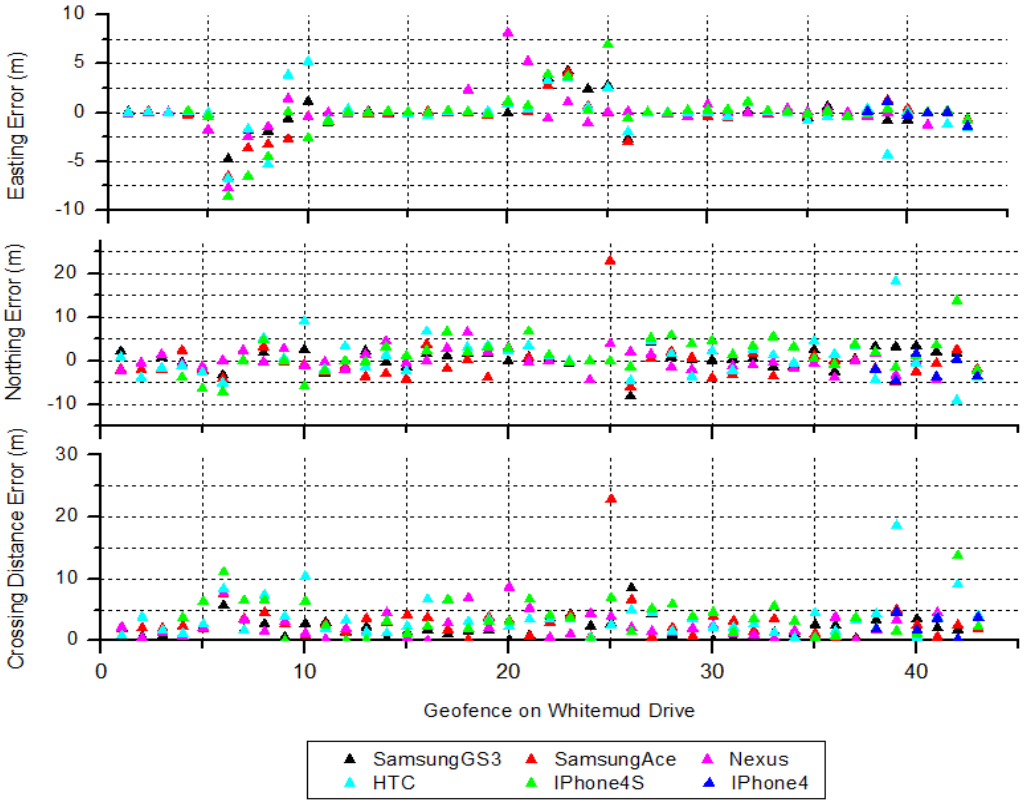

Figure 30 Plot of freeway distance error

The first two plots present the discrepancy of the easting and northing coordinates along Whitemud drive, and the third plot shows the horizontal discrepancy. Geofence 1 to 15 and 38 to 43 are deployed in the westbound direction, and 16 to 37 are deployed in the eastbound direction. Geofence 5 to 10 and 21 to 26 are in the north-south direction, and rest of the Geofences are in the east-west direction. The first two plots show that at locations where easting error is small, the northing error is relatively larger, and vice versa. At the Geofences that are deployed in the east-west direction, the easting error is close to 0, and at the Geofences that are deployed in the north-south direction, the easting error

becomes much higher. On the other hand, the northing error is smaller at the Geofence locations in the north-south direction, and it is larger at the locations in the east-west direction. These trends indicate that the discrepancy in the longitudinal direction of travel is much smaller than that in the transverse direction. So estimation of traffic measures along longitudinal direction will be more accurate than those in transverse direction. Figure 31 shows the box plot of the distance discrepancies.

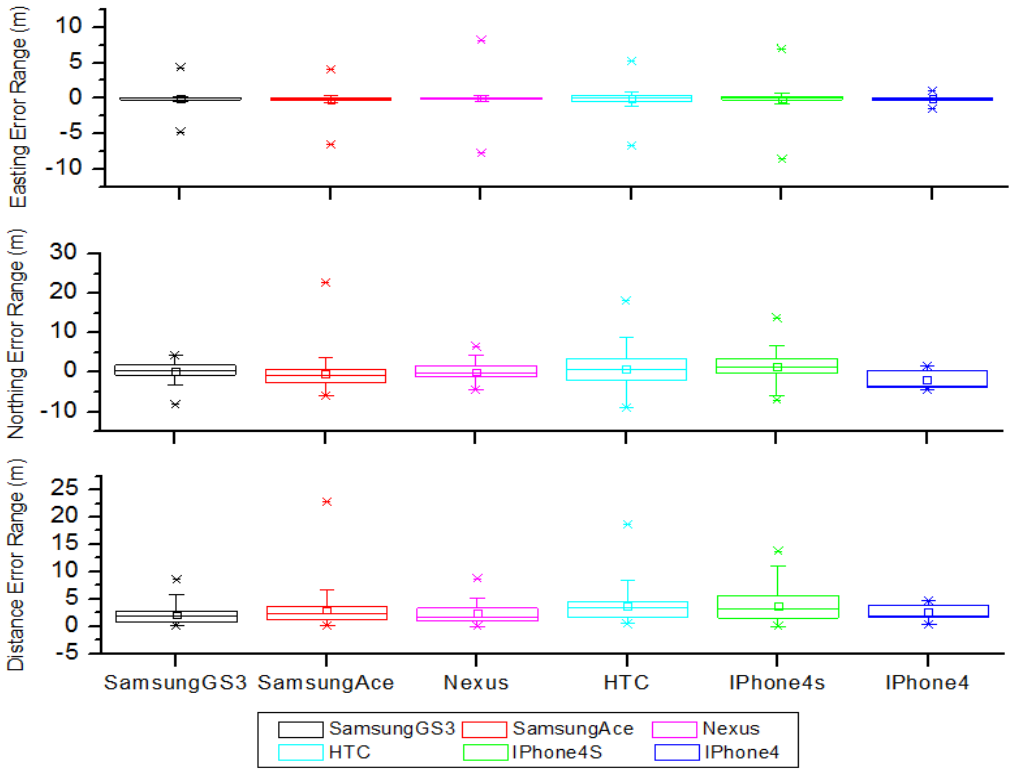

Figure 31 Box plot of freeway distance error

All smartphones have similar range of positioning errors. For easting error, the magnitudes are all close to 0, and Android smartphones have more outliers than the iOS smartphones. For northing and horizontal distance error, the plots for first three Android phones show that the lower quartile and upper quartile of the

error distribution are closer to the median compared to the last two Android smartphones. For the last iOS smartphone, the median value of the horizontal position error is very close to the lower error quartile.

The average absolute easting, northing and horizontal error of location estimation at Geofences are listed in Table 15. The average easting error is less than northing error because most of the Geofences are deployed in the east-west direction, and the error in the transverse direction is greater than that in the longitudinal direction.

Table 15 Location error at Geofence crossing along Whitemud Drive

	Easting Error	Northing Error	Horizontal Error
Total	0.95	2.45	2.97
Android	0.78	2.17	2.20
iOS	1.07	3.03	3.63

The scattered plot for the timestamp differences at crossing the reference lines in Geofences is shown in Figure 32 below. Most differences in timestamp are scattered near the Y=0 axis within the boundary of -1 s and 1 s. This indicates that when a vehicle crosses a reference point, the crossing timestamp can be recorded by the smartphone GPS and Geofence to the accuracy of within 1 second. Five out of six smartphones performed well in data collection, however, IPhone 4 encountered some problem and only captured six data points near the end of the trip, and all six timestamp errors are all below -1.

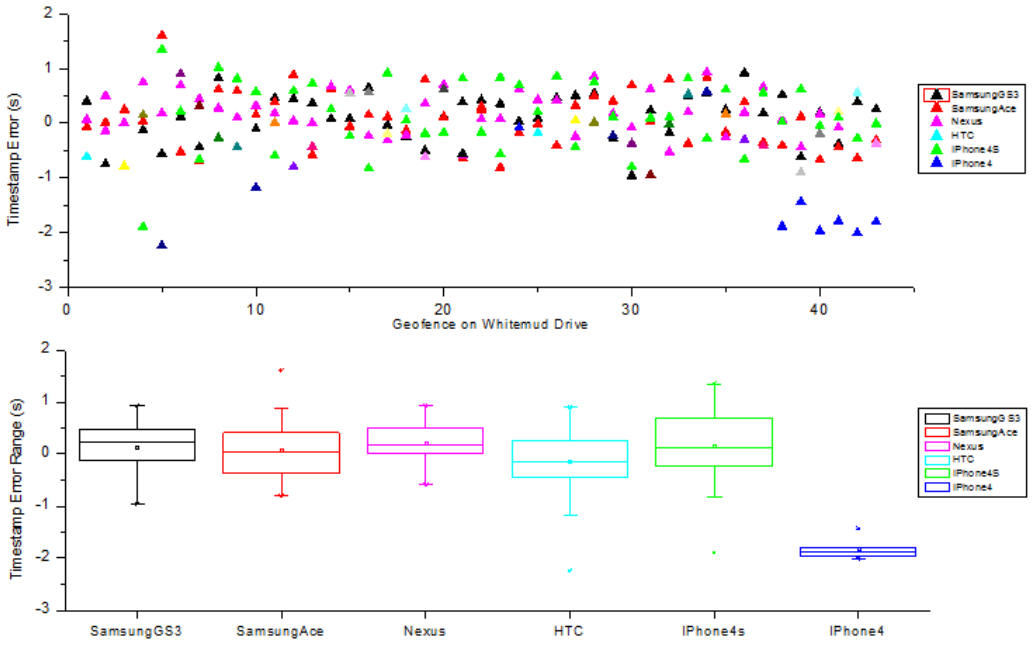

Figure 32 Plot of freeway timestamp error

The average absolute Δtimestamp for all the Geofence crossings and all the smartphones is 0.47seconds, the average value for android phones is 0.41 second and the average for iOS phones are 0.69 seconds.

The calculated and ground truth link travel times between two consecutive Geofences are compared and the difference is calculated and plotted in Figure 33. Most of the ΔT_{link} value ranges within 1.5 s above and below 0. The mean absolute ΔT_{link} for all the smartphones is 0.61s, for Android smartphones is 0.57s and for iOS phones is 0.75s. The difference in total travel time on Whitemud drive is ΔT_{path} =0.14s, ΔT_{path} = -0.31 s in the westbound direction and ΔT_{path} =0.17s in the eastbound direction. The positive and negative errors resulting from the overestimation and underestimation of the link travel time may cancel each other and hence result in a lower overall error.

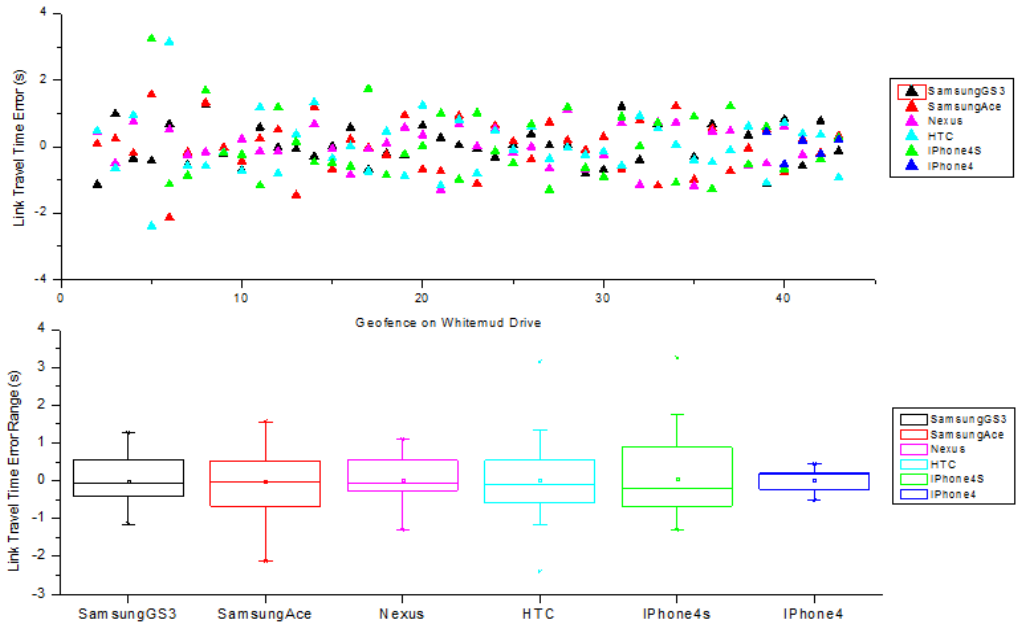

Figure 33 Plot of freeway link travel time error

The calculated and ground truth average link travel speed between the two consecutive Geofences are also compared, the difference is calculated and plotted in Figure 34.

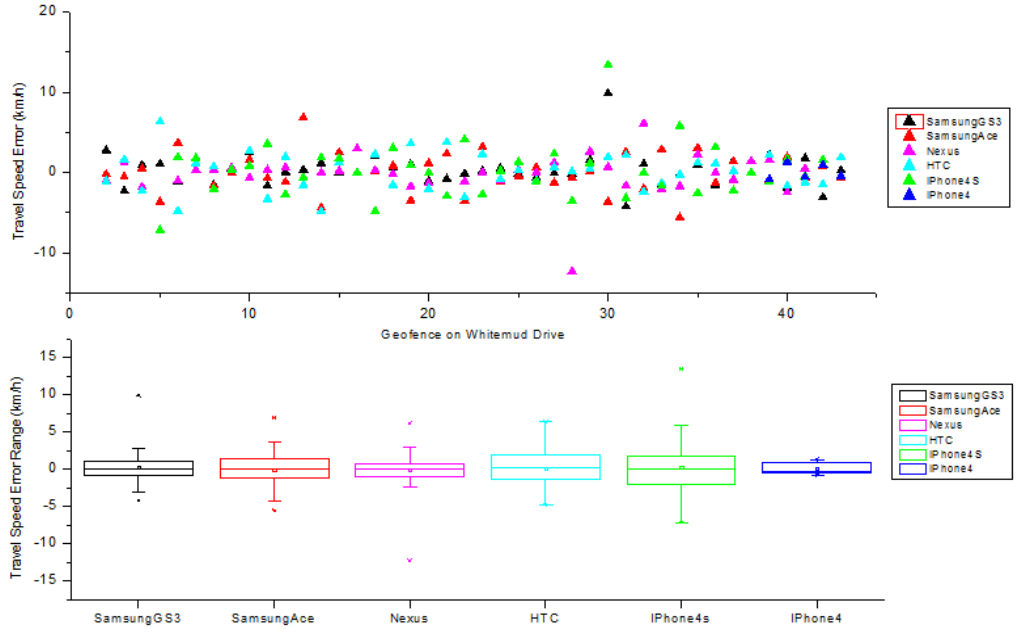

Figure 34 Plot of freeway average link travel speed error

Most of the speed discrepancies are within the range of ±5 km/h. HTC and IPhone4S have higher range of errors, and Nexus has least error. The overall Δv_{link} has mean of 1.72 km/h. For Android smartphones Δv_{link} =1.61 km/h and for iOS phones, Δv_{link} =2.14 km/h.

All the Geofence crossing mean squared errors are plotted together with smartphones in Figure 35. The comparison between the Android and iOS phones are carried out using the relative error data from two iOS smartphones and two of the Android smartphones. The data from the two Android smartphones with least and greatest relative error are excluded from the comparison. Comparing the errors among smartphones, SamsungGS3 and Nexus have higher errors than other smartphones, and IPhone4 has the lowest error. Samsung Ace has the highest absolute timestamp error and lowest absolute link travel time error and absolute average speed error.

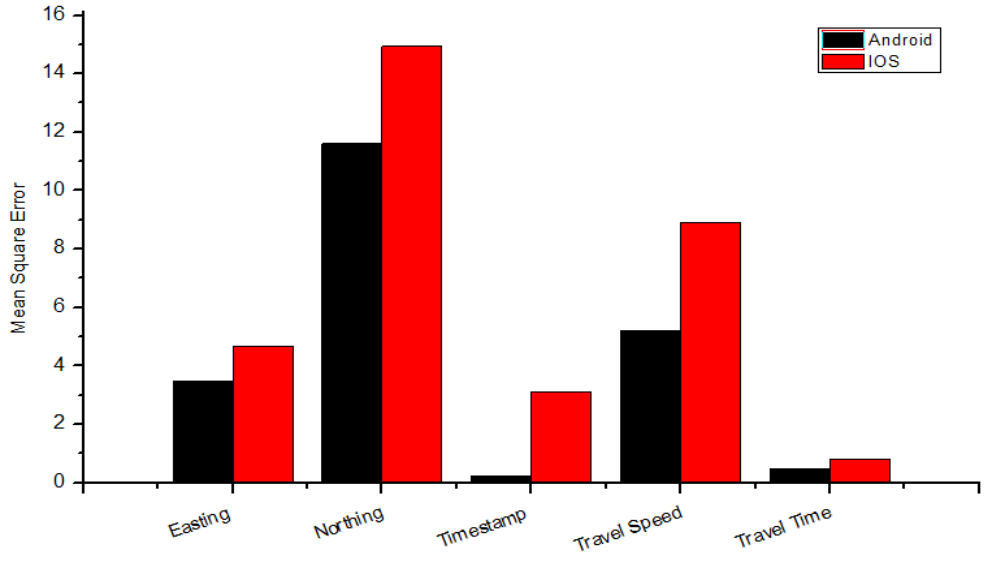

Figure 35 Plot of freeway Geofence crossing errors with smartphones

4.3.2 170 Street

The section of 170 Street traversed during the experiment is between 87 Avenue and 118 Avenue. Ten Geofences were deployed at downstream of the intersections in each travel direction. The deployment locations are shown in Figure 36.

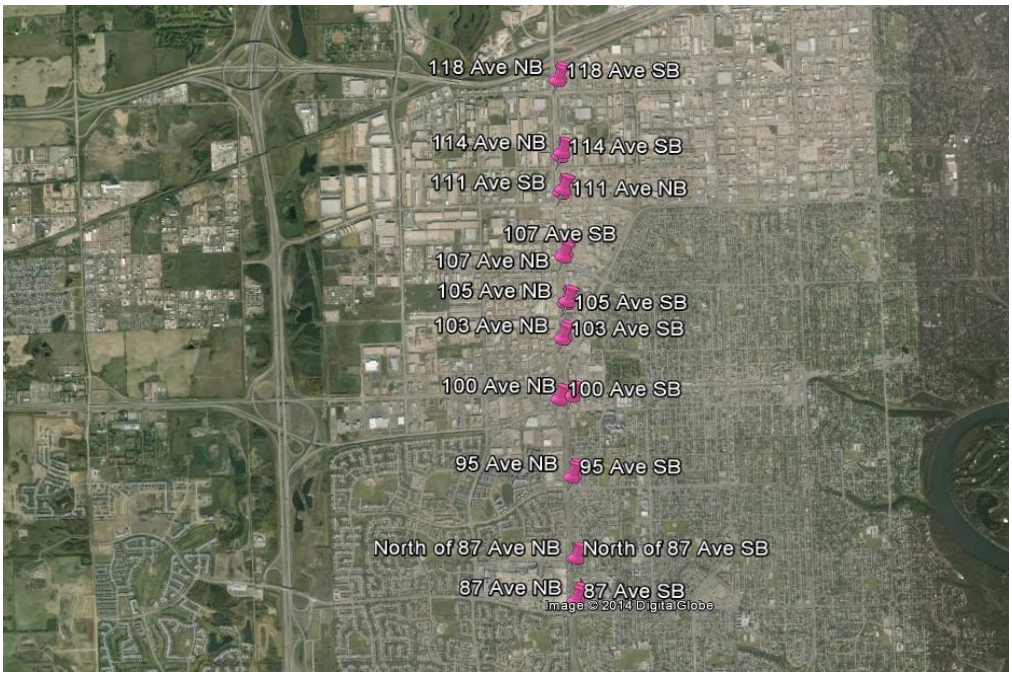

Figure 36 Deployment location of Geofences on 170 Street

The timestamp and location of when and where the vehicle traverses the Geofences were recorded and compared to the ground truth timestamp and locations. The crossing location discrepancies in the easting and northing error are presented in Figure 37 below. The first two plots present the location discrepancy in the easting and northing directions along the 170 streets, and the third plot shows the horizontal discrepancy.

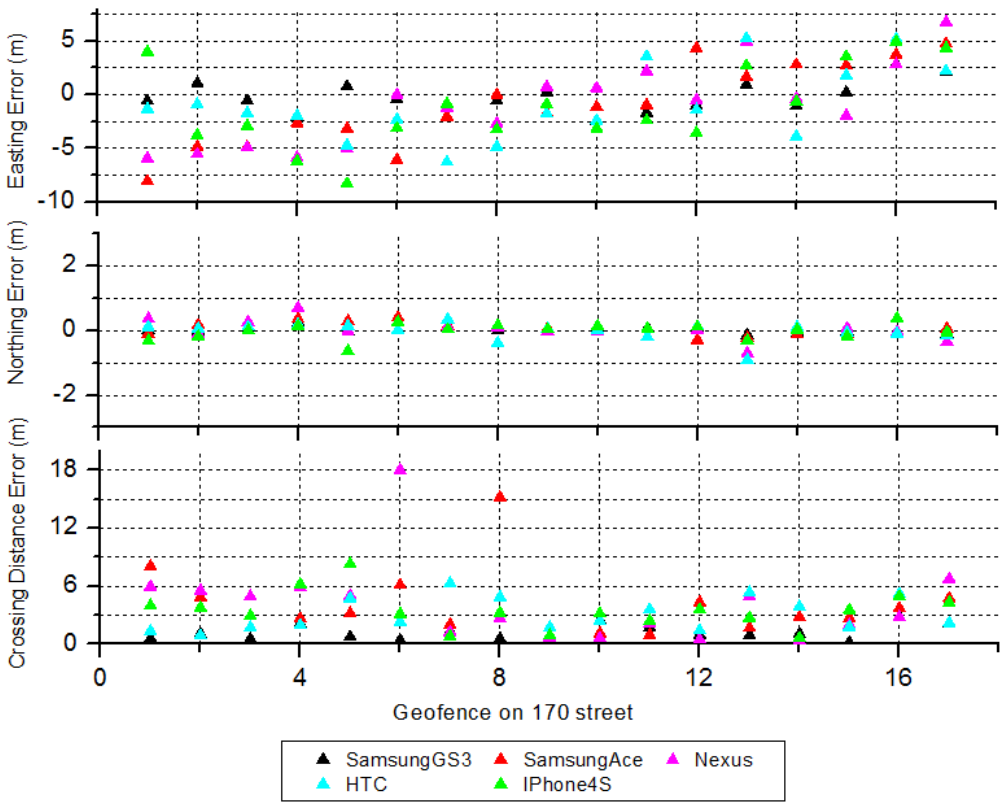

Figure 37 Plot of arterial distance error

Similar to what have been discussed in the last section, as the vehicle travels in the north-south direction, the position error at Geofence crossing in the northing direction will be smaller than that in the easting direction. In this case, the vehicle was travelling along 170 Street in the north-south direction, and the northing error is within ±1 m for all the smartphones, and the easting error varies between -10 m to 5 m.

The average absolute easting, northing and horizontal error of location estimation at Geofence are listed in Table 16. In this case, the vehicle was travelling in the north-south direction, so the average easting error is greater than the average northing error for all cases.

Table 16 Location error at Geofence crossing along 170 street

	Easting Error	Northing Error	Horizontal Error
Total	2.79	0.54	3.19
Android	2.63	0.63	3.13
iOS	3.44	0.18	3.44

The easting and horizontal error of Android smartphones are less than that of iOS smartphones. In general, all three errors captured along this arterial street are greater than the error captured on the freeway segments.

The scattered plot for the timestamp differences at Geofence crossing is show in Figure 38 below. Most differences in timestamp are within the ±1.5 s range from the ground truth. No specific trend is observed from the scattered plot.

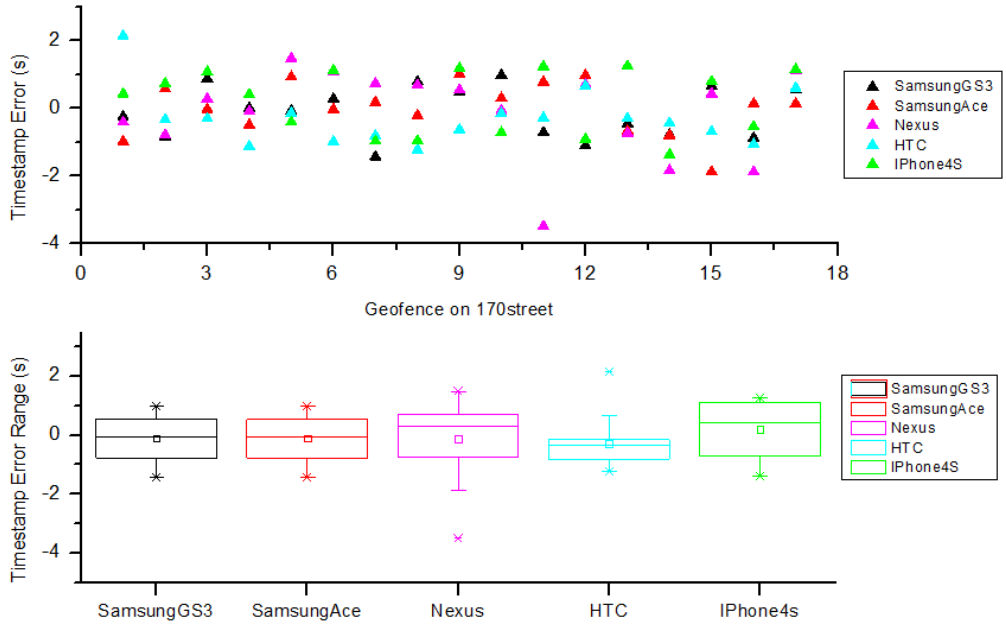

Figure 38 Plot of arterial timestamp error

The average absolute timestamp error at crossing the Geofences deployed on 170 Street is 0.76 s, the average absolute timestamp among Android phones is

0.73s, and that for iOS smartphones is 0.90 s. The box plots show that HTC has the smallest range of relative error, and IPhone 4s has the greatest range.

The calculated and ground truth link travel times between any two consecutive Geofences are compared and the difference is calculated and plotted in Figure 39. Most of the link travel time errors are within -3 s to 2.5 s range. The mean absolute link travel time error for all smartphones is 1.07 s, for Android phones is 0.98 s, and for iOS phones is 1.42 s. The difference in total travel time on 170 Street is ΔT_{path} =2.78s in both directions, ΔT_{path} =1.03s in the northbound direction and ΔT_{path} =1.75s in the southbound direction. In this box plot, all the error ranges are greater than the ranges on Whitemud Drive. In both freeway and arterial scenarios, the error range for IPhone4s is the greatest among all the phones.

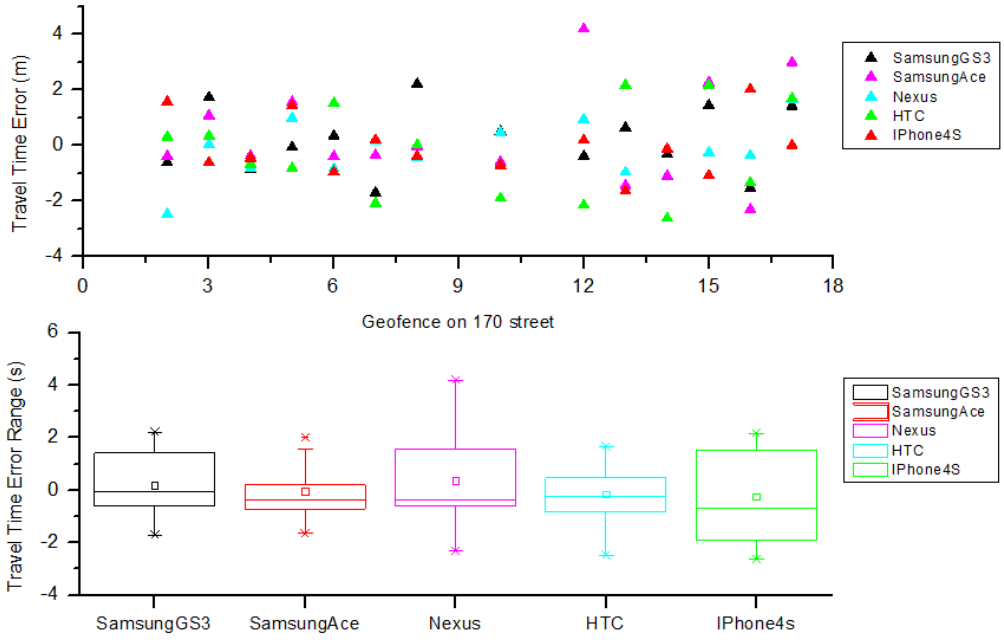

Figure 39 Plot of arterial link travel time error

The calculated and ground truth average link travel speeds between two consecutive Geofences are compared and the differences are calculated and plotted in Figure 40. Most speed discrepancies are within the range of ±6 km/h. From Geofence 2 to Geofence 7, the travel speed estimates for all the phones are close to each other; from Geofence 8 to Geofence 12, the difference of travel speeds between smartphones grow larger, and from Geofence 13 to the last Geofence, the differences in error reduced again. For Android smartphones the absolute speed error is 1.12 km/h, and for iOS smartphones the average error is 1.87 km/h.

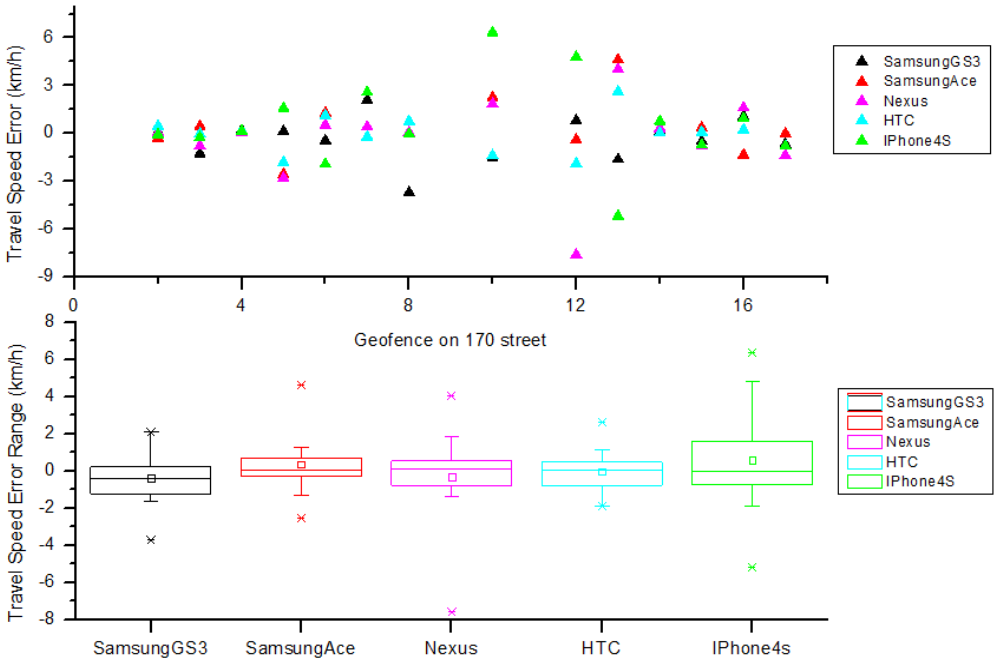

Figure 40 Plot of arterial average link travel speed

4.3.3 Comparison to loop detectors

The section of Whitemud Drive between 122 Streets to 170 Street is equipped with inductive loop detectors on both directions. These point based sensors are pre-programmed to report aggregate traffic measures at 20 s time intervals, including vehicle count, time mean speed and occupancy. The approximate locations of the loop detectors are labelled in Figure 41 below. The numbers in blue boxes indicate the detectors in the westbound direction, and those in pink boxes indicate the detectors in the eastbound direction.

Figure 41 Loop detector deployment along Whitemud Drive

The average link travel speeds measured by the smartphones and Geofences were calculated using the distance travelled between the two consecutive Geofences dividing by the time travelled between the two Geofences. This assumes that the vehicle was travelling at a uniform speed over the entire link. The loop detector point speeds were used to linearly interpolate the point

speeds at Geofence locations, and the measured link travel speed using Geofence was matched with the interpolated loop detector point speed during the 20-second time interval coinciding with the approximate time that the vehicle passed over the loop detector. The point speed estimate at the Geofence locations and loop detector locations are presented in Figure 42.

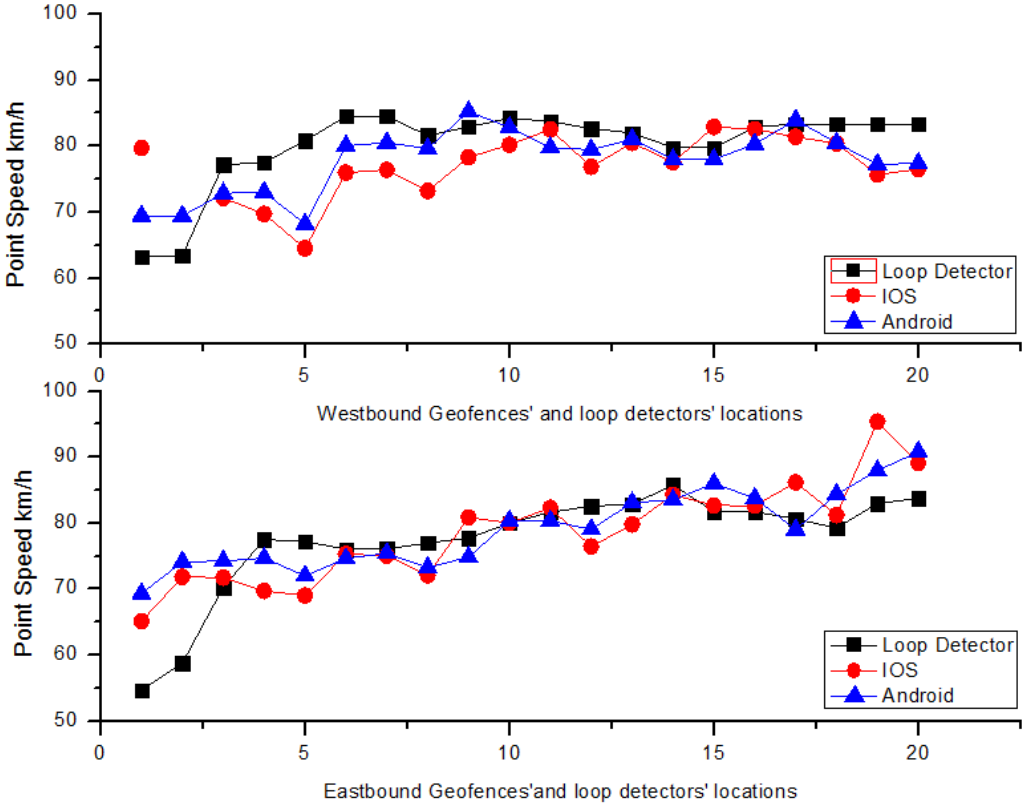

Figure 42 Plot of interpolated point speed on Whitemud Drive

In the westbound direction, at most locations, the point speed estimate from loop detectors are higher than that from Geofences, and the Android smartphones' speed estimation is higher than the speed estimation from the iOS smartphones. In the eastbound direction, the point speed estimates from loop detectors and Geofences are similar. In both cases the estimates from iOS smartphones fluctuate more than other two speed estimates. In both directions, the

loop detector speed estimates are more continuous where the Geofence estimated speed has more fluctuation. The box plot of the westbound and eastbound point speed estimation errors are presented in Figure 43 below.

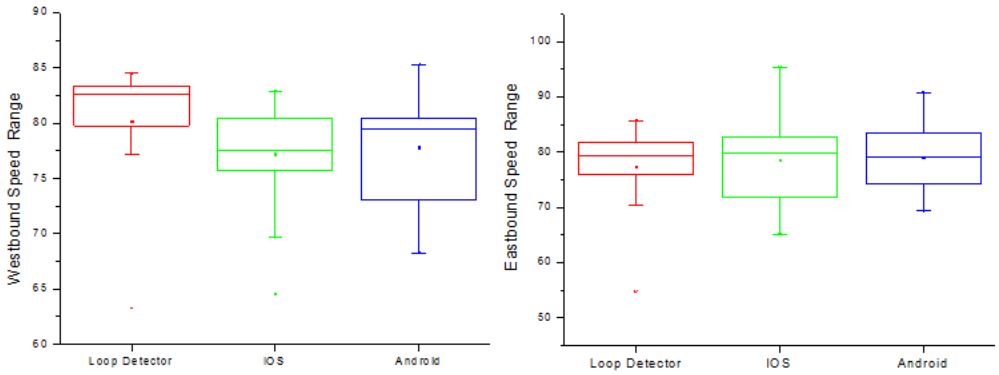

Figure 43 Box plot of interpolated point speed on Whitemud Drive

In the westbound direction the estimated median point speed using loop detector data is around 82.5 km/h, and the lower and upper quartile covers speed from 80 km/h to 83 km/h. The speed estimate from iOS smartphone GPS has median of 77.5 km/h, and the estimate from Android smartphones' GPS has median of 80 km/h. The estimation from Geofence data captures a greater range of speeds. Similarly, in the eastbound direction, speed estimation from smartphone and Geofence data have greater range, but the median speed estimation from both loop detector data and Geofence data are very close in this case.

The loop detector interpolated point speed is also used to estimate the link travel time, and its comparison to the Geofence estimated link travel time and ground truth link travel time are plotted in Figure 44. The loop detector order is from 1 to 18, where the first 9 are the detectors in the westbound direction, and the rest 9 are the detectors in the east direction.

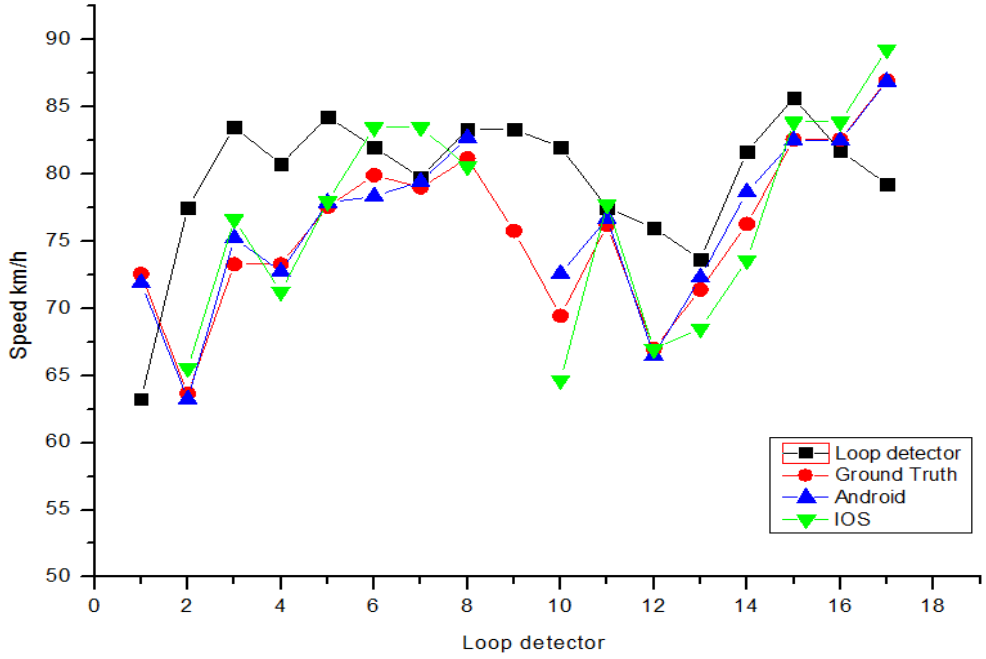

Figure 44 Plot of link travel speed with loop detectors

The plot shows that average link travel speed estimated using Android smartphone and Geofence is close to the ground truth data, the estimated speed obtained using IOS phones are less accurate than Android phones. The mean difference between link travel speeds are shown in Table 17. The mean link travel speed discrepancy for Android smartphones is 1.27 km/h which is the lower than that of iOS smartphones. Both Figure 44 and Table 17 show that using the loop detector interpolated point speed to estimate the link travel time cannot well represent the link travel speed between the Geofences.

Table 17 Difference in segment speed between loop detectors and smartphone GPS

	Loop Detectors	Android GPS	iOS GPS
Mean	6.31	1.27	2.16
Standard Deviation	4.03	1.30	1.48
Range	0.74-13.85	0.02-6.82	0-4.80

Loop detectors and Geofence measurements differ from each other and level of discrepancy varies with time, location, traffic conditions etc. Loop detectors and Geofences both compute instantaneous velocity, however in different ways. Dual loop detectors use the travel time between dual coils to compute the speed for the passing vehicles. The distance between the two coils is pre-determined, and the travel time between the two coils is determined by the detection signals of the loops. This point speed is often used to represent the ground truth speed. If loop detector at a location provides biased estimates due to error and defects, there is no efficient way to check and reinforce the reliability of the estimation at that location, and all the traffic information at that point may be missing.

Geofence uses GPS data points to compute the velocity. Two GPS location points with corresponding timestamps collected within a Geofence are used to estimate the distance and travel time between the two points. The distance and travel time varies between trajectories and are highly depended on GPS signal reception. If GPS signal is not received during the time when a vehicle traverses cross the Geofence, no traffic information will be collected at this location. However, since the cost for Geofence deployment is low, consecutive Geofences

can be set up at near upstream and downstream of the location to help capturing the missing information. In addition, if the Geofences are deployed as closely paired sensors, with supporting algorithms, its functionality can be easily expanded to not only capturing vehicle speed, but also, volume, density, headway and occupancy.

Although loop detectors can provide relatively accurate information at fixed points, their performance in estimating the traffic state parameters along the longer corridor is questionable. The cost for installation and maintenances are usually high, and these operations also create disturbance to the adjacent traffic, hence, additional cost may be imposed onto the road users. In addition, the operation of the fixed sensors like loop detectors, video cameras are more susceptible to the ambient environment such as cold weather and high grass. All these concerns limits it's capability of providing spatially continuous traffic information over the monitored network. Opposed to that, Geofence not only can provide accurate information at fixed points, but also can provide cost efficient solutions that are economically feasible and are less susceptible to operation environment.

As there is a rapidly growing interests in moving away from fixed sensor such as loop detectors to tracking probe vehicles such as deployment of Geofence and smartphone GPS, some concerns may raise. One is that Geofences collect velocity from a proportion of vehicles crossing that location while loop detector stations collect data from all the passing vehicles. If the penetration rate of using the GPS-enabled smartphones with Geofence related applications is small, it

might not be statistically representative of the entire population. In addition, Geofence only captures traffic data from GPS-enabled smartphones with Drivewyze or equivalent application, the captured population only represents the group of drivers that uses such more advanced cellular phones. These drivers may be more representative of the younger generation, and the driver behavior may exhibit a specific bias. Hence, although using the GPS-enabled smartphone and Geofence for traffic data capturing is promising in perspectives of non-intrusive, high accuracy, and cost effectiveness, more research has to be carry forward to evaluate the data reliability and investigate the unsolved issues.

CHAPTER 5. CONCLUSIONS AND RECOMMENDATIONS

This chapter presents the summary of major findings and contributions of this study, and discusses the research limitations, as well as puts forward some recommendations for the future works.

5.1 Research Summary

In this study, field experiments were designed and conducted along freeway, highway, and urban arterials in the City of Edmonton to collect the probe location data using different technologies/devices. The data collection was performed using professional GPS handset, GPS-enabled smartphones, video camera and Geofences. The experiment was carried out as three scenarios to estimate the relative positioning error of using GPS-enabled smartphones, cellular networks, and combination of the smartphone and Geofences. The characteristics of positioning error were described, and the relationships between the error and traffic attributes were investigated through regression analysis. Algorithms were designed to collect and estimate useful traffic state information using the combination of the smartphones and Geofences. The quality of estimated traffic state parameters was evaluated and compared to ground truth data and inductive loop detector data, and the performance of different devices were also discussed.

5.2 Research Findings

The following research finding can be concluded from the field observation and result analysis:

- Comparing the professional GPS handset data with the smartphone GPS data, the mean relative easting and northing error are in the range of ±1 m. For most cases, 95% of the relative horizontal error was within a 0-10 m range. Projecting vehicle trajectory to Google Earth, 92% of the data points are correctly positioned on the roadway segments, and an average coverage of 36 points per kilometer was observed.
- Using the cellular positioning technique, the average relative positioning error in the easting and northing direction are between 1m to 10 m, and the average relative horizontal error is around 56 m. Although by using the cellular positioning technique the tested smartphone application can record the cell-ID along the test segment in repeatable trials, the positioning accuracy is much lower than that of using GPS-enabled smartphones.
- Use the combination of GPS-enabled smartphone and Geofence the average relative poisoning error for the data collected within the Geofences are less than 10 m. This accuracy level is comparable to positioning using GPS-enabled smartphone alone; however use of Geofence will save much of battery by only recording the position data within the Geofence area.
- In all scenarios, use GPS-enabled smartphones, cellular probes and Geofence for obtaining location information is feasible and cost effective;

and particularly, using GPS-enabled smartphones and its combination with Geofences will provide better location accuracy, and more useful traffic state information.

- The observed relative positioning error from smartphones follows lognormal distribution. All the explanatory variables considered in the multivariable regression analysis are highly significant, and these variables accounts for 24% of the variation in the relative positioning error. The relative positioning error collected using GPS-enabled smartphones on urban arterials are greater than that collected on highway and freeway. The position data collected by bus has greater error than the data collected by using passenger car. When holding other factors constant, with mobile network enabled, the positioning error may reduce 28%, and with limited sight to the satellites, the positioning error may increase 40%. Increase of speed will lead to increase of error. The impact of speed on positioning error increases when the speed increases between 20 km/h to 60 km/h, and the impact decreases as speed increases from 60 km/h to 90 km/h. The positioning error for data collected when travelling at speed range of 100 km/h to 110 km/h is the highest compared to travelling at all other speeds between 0 km/h to 140 km/h.
- When estimating the traffic state parameters, the horizontal position error at reference line crossings in the longitudinal direction of travel is much smaller than that in the transverse direction. The timestamp error and the link travel time error are mostly within the range of ±1 s. The average link

travel speed error is within the range of ±5 km/h. For the data collected on urban arterials, the horizontal position error, timestamp error, and link travel time error are greater than those collected on freeway segments. However, the link travel speed error for the data collected on the arterials is smaller than that collected on freeway.

- When estimating the point speed along freeway segments, Geofence is capable of capturing a greater range of speed than the loop detector does, and the Geofence captured point speed is close but slightly lower than loop detector interpolated point speed. In comparison to the ground truth link travel speed, the link travel speed estimated using Geofence data has smaller discrepancy, and the loop detector estimated link travel speed is generally higher.
- Comparing the smartphones' performance on location estimation, the position data collected by Android smartphones has higher accuracy than that collected by using iOS smartphones. The mean network delay for all the smartphones is around 6.64 s, the delay experienced by iOS smartphones is less than that for Android smartphones, and the Android smartphones has higher detection rate than the iOS smartphones. When estimating traffic state parameters, Android smartphones has better performances than iOS smartphones in most cases.

5.3 Limitation of this study

The experiment conducted in this study only covers one highway, one freeway and several urban arterials, and deployment of Geofence was only on two corridors, so the position data may not be representative in all the cases. The smartphones used in the experiments are not representative of all other phones and the specifications of the GPS chips in the phones are not known. It is expected that more data collection on variety types of roads by different vehicles and devices would certainly have better results.

The proposed methodology for traffic states estimates are performed after the field experiments, however, the position data from the Geofence can be sent to the server through wireless communication which provides the possibility of real-time implementation of the traffic detection, traffic states and error computation. A systematic real-time algorithm may be developed to automatically calculate the parameters which will reduce time for analysis and reduce human errors.

5.4 Future work and recommendation

The conclusion of this work indicates that the relative positioning error of GPS-enabled smartphones is affected by several traffic related factors. However there must be other contributing factors not captured in this study. More field experiments may be carried out in future researches to include more factors such as different weather and different traffic conditions in the multi-variable regression analysis to generate better model estimates. For example the meteorology conditions at the time of the field test may lead to some variability of

the positioning error, and factor of meteorology may be considered in the future studies.

Although the data set in this study is large, a power analysis was not conducted for the statistically analysis. It is recommended that in future studies, this part of the analysis can be included to validate the significance of the effective size. In addition, the transformation error in the process of converting coordinates to different systems may be calculated in mathematical form, and be filtered out from the overall positioning error to produce more accurate accuracy level estimation.

Since it is feasible to combine the GPS-enabled smartphones with Geofence in traffic data capturing, a strategy for wider deployment of Geofence as well as data fusion technique may be developed. If there is enough penetration rate, combination of smartphone and Geofence may be used in real-time traffic state prediction, and other traffic states parameters such as density, headway and occupancy may be estimated using this approach. For ITS applications, the Geofence can be set up to cover weaving segments which can help identify the weaving patterns and ramp metering strategies. For safety applications, the consecutive Geofences may be able to capture the traffic conditions at close upstream and downstream of the incidents thus provide the road users with better crash pattern estimates and post-incident management strategies. The algorithms for using combination of GPS-enabled smartphones and Geofence for such applications may be researched in future studies.

REFERENCES

[1] Michiel, Minderhoud M.; Hein, Botma; Piet, Bovy H.L., "Assessment of Roadway Capacity Estimation Methods," *Transportation Research Record: Journal of the Transportation Research Board,* vol. 1572, no. 1, pp. 59-67, January 1997.

[2] Bell, Katherine E; Figliozzi, Miguel A, "Evaluation of smart phone weight-mile tax track data for supporting freight modeling, performance measures and planning," in *Transportation Research Board 92nd Annual Meeting*, Washington, D.C., 2012.

[3] Shladover, Steven E; Tan, Swe-Kuang, "Analysis of vehicle positioning accuracy requirements for communication-based coorperative collision warning," *Journal of Intelligent Transportation Systems: Technoloy, Planning, and Operations,* vol. 10, no. 3, pp. 131-140, Jan 2007.

[4] "comScore," 2013. [Online]. Available: http://www.comscore.com/. [Accessed 15 July 2013].

[5] Farrell, J; Barth, M, The global positioning system and inertial navigation, vol. 61, NY: McGraw-Hill New York, 1999.

[6] Farrell, J A; Givargis, T D; Barth, M J, "Real-time differential carrier phase GPS-aided INS. Control Systems Technology," *IEEE Transactions on,* vol. 8, no. 4, pp. 709-721, 2000.

[7] E. H. Trinklein, "Post processing of multiple gps receivers to enhance

baseline accuracy," 2011.

[8] L. Klein, Traffic Detector Handbook: Third Edition, Washington, D. C: U.S. Department of Transportation, 2006.

[9] Turner, S. M., W. L. Eisele, R. J. Benz and D. J. Holdener., "Travel time data collection handbook. FHWA-PL-98-035. FHWA," Federal Highway Administration, Office of Highway Information Management, Washington, D. C, 1998.

[10] B. R. Hellinga, "Improving Freeway Speed Estimates from Single-Loop Detectors," *Journal of,* vol. 128, pp. 58-67, 2002.

[11] Park, S., and Ritchie, S. G., "Innovative Single-loop Speed Estimation Model with Advanced," *IET Intelligent Transport Systems,* vol. 4, pp. 232-243, 2010.

[12] Turner, S. M., W. L. Eisele, R. J. Benz and D. J. Holdener., "Travel time data collection handbook," Federal Highway Administration, Office of Highway Information Management, Washington, D. C, 1998.

[13] Schuessier, Nadine; Axhausen, Kay W, "Processing raw data from global positioning systems without additional information," *Transportation Research Record: Journal of the Transportation Resaerch Board,* no. No.2105, pp. 28-36, 2009.

[14] P. A. Zandbergen, "Accuracy of Iphone Locations: A comparison of assisted GPS, wifi and cellular positioning," *Transactions in GIS,* no. 13, pp. 5-26, 2009.

[15] Ratti, C., Frenchman, D., Pulselli, R. M., & Williams, S., "Mobile Landscapes: using location data from cellphones for urban analysis.," *Environment and Planning B: Planning and Design,* pp. 33,727,748, 2006.

[16] J. C. Herrera, "Assessment of GPS-enabled smartphone data and its use in traffic state estimation for highways," 2009.

[17] G. Rose, "Mobile phones as traffic probes: practices, prospects and issues," *Transport Reviews,* vol. 26, no. 3, pp. 275-291, 2003.

[18] W. Lee, Wireless and CellularCommunications 3rd Edition, New York: McGraw-Hill Professional, 2005.

[19] Yang, F; Cheng, Y; Jin, J; Yang, D; Ran, B, "Wireless communication simulation model for dynamic cellular handoff-based traffic monitoring systems: framework and evaluation," *Transportation Resaerch Board 91st Annual Meeting,* 2012.

[20] B. Hillel, "Evaluation of a cellular phone-based system for measurements of traffic speeds and travel times: a case study from Israel," *Transportation Research Part C,* vol. 15, pp. 380-391, 2007.

[21] Z. Qiu, "Macroscopic traffic state estimation for large scale freway network using wireless network data," PH.D. dissertation, University of Wisconsin Madison, Madison, 2007.

[22] Gundlegerd, D., J.M.Karlsson, "Handover location accuracy for travel time estimation in GSM and UMTS," *IET Intelligent Transportation System,* vol. 3, pp. 87-94, 2009.

[23] I. T. Union, 2011. [Online]. Available: http://www.itu.int/ITU-D/ict/statistics/ict/index.html. [Accessed July 2013].

[24] Mohr, M, "A study of LBS accuracy in the UK and a novel approach to inferring the positioning technology employed," *Computer Communications 31,* pp. 1148-1159, 2008.

[25] Sanwal, Kumud K., J. Walrand, "Vehicle as Probes," Institute of Transportation Studies, University of California Berkeley, Berkeley, 1995.

[26] H. Bar-Gera, "Evaluation of a cellular phone-based system for measurements of traffic speeds and travel times: A case study from Israel," *Transportation Research Part C,* vol. 15, pp. 380-391, 2007.

[27] Ygnace, Jean-Luc; Drane, Chris; Yim, Y B; de Lacvivier, Renaud, "Travel Time Estimation on the San Francisco Bay Area Network Using Cellular Phones as Probes," 2000.

[28] Parkinson, B, "A History of Satellites Navigation.," *Journal of hte Institute of Navigation,* vol. 42, pp. 109-164, 1995.

[29] Zumbergeand, W; Bertiger, W, "Global Positioning System: Theory and Applications," *Progressin Astronautics and Aeronautics,* vol. 163, pp. 585-599, 1996.

[30] M. C. Olynik, "Temporal characteristic of gps error sources nad their impact on relative positioning," Calgary, 2002.

[31] Meaker, J.,M.W.Horner, "Use of automatic position reporting system data for enhancing transportation pallning operations," *Transportation Research*

Record: Journal of the Transportation Research Broad, no. 1870, pp. 26-34, 2004.

[32] Byon, Y.J., Shalaby, A., and Abdulhai, B. , "GISTT: GPS-GIS Integrated System for Travel Time Surveys.," in *Transportation Research Board*, Washington, D.C., 2006.

[33] Krause, A., Horvitz, E.,Kansal,A., Zhao, F., "Toward Community Sensing," in *International Conference on Information Processing in Sensor Networks*, St Louis, 2008.

[34] Nanthawichit, C., Nakatsuji, T., and Suzuki, H., "Application of Probe-Vehicle Data for Real-Time Traffic-State Estimation and Short-Term Travel-Time Prediction on a Freeway.," *ransportation Research Record: Journal of the Transportation Research Board,* vol. 1855, pp. 45-59, 2003.

[35] Herrera, J. C., Andrews, S., Apte, S., Arnold, J., Ban, J., Benko, M., Bayen, A. M., Chiou, B., Claudel, C., Claudel, C., Dodson, T., Elhamshary, O., Flens-Batina, C., Gruteser, M., Amin, S., Herring, R., Hoh, B., Jacobson, Q., Kumar, M., Iwuchukwu, T., L, "Mobile Century - Using GPS Mobile Phones as Traffic Sensors: A Field Experiment," in *ITS America*, New York, NY, 2008.

[36] Herrera, J. C., and Bayen, A. M., "Incorporation of Lagrangian Measurements in Freeway Traffic State Estimation.," *Transportation Research Part B: Methodological,* vol. 44, no. 4, pp. 460-481, 2010.

[37] Aguilar, David P; Barbeau, Sean J; Labrador, Miguel A; Perez, Alfredo J;

Perez, Rafael A; Winters, Philip L, "Quantifying Position Accuracy of Multimodal Data from Global Postioning System-Enabled Cell Phones," *Transportation Research Record:Jounal of the Transportation Research Board,* vol. No. 1992, pp. 54-60, 2007.

[38] Yim, Y B; Cayford, Randall, "Investigation of Vehicles as Probes Using Global Positioning System and Cellular Phone Tracking:," 2001.

[39] Trimble, "Juno Series," 2013. [Online]. Available: http://www.trimble.com/. [Accessed 5 July 2013].

[40] Kern, W.F. and Bland, J.R., Solid Mensuration with Proofs, New York, 1948.

[41] H. Steinhaus, in *Mathematical Snapshots*, New York, 1999, pp. 220-221.

[42] K. Grade, "A non-singular horizontal position representation," *The Journal of Navigation,* vol. 63, pp. 395-417, 2010.

[43] "Calculate distance, bearinga nd more between Latitude/Longtitude points," [Online]. Available: http://www.movable-type.co.uk/scripts/latlong.html. [Accessed 2 June 2013].

[44] Dennis J. Beal, Science Applications International Corporation, Oak Ridge, TN, "Information Criteria Methods in SAS for Multiple Linear Regression Models," in *SESUG*, Hilton Head, 2007.

[45] van Lint, J. and N. van der Zijpp, "Improving a travel time estimation algorithm by using dual loop detecors," *Transportation Research Record: Journal of hte Transportation Research Board,* vol. 1855, pp. 41-48, 2003.

[46] Kothuri, S.M., K.A.Tufte, S. Ahn and R.L.Bertini, "Toward understanding and reducing errors in real-time estimation of travel times," *Transportation Research Record: Journal of the Transportation Research Board,* vol. 2049, pp. 21-28, 2008.

[47] Sun, L. J. Yang and H. Mahmassani, "Travel time estimation based on piecewise truncated quadratic speed trajactory," *Transportation Research Part A,* vol. 42, pp. 173-186, 2008.

[48] Li, R., G. Rose and M. Sarvi, "Evaluation of speed-based travel time estimation models," *ASCE Journal of Transportation Engineering,* vol. 132, no. 7, pp. 540-547, 2006.

[49] E. Kwon, "Development of operational strategies for travel time estimation and emergency evaluation of freeway network," Minnesota Department of Transportation, State of Minnesota, 2004.